von KARMAN INSTITUTE

FOR FLUID DYNAMICS

TECHNICAL NOTE 112

KINETIC THEORY DESCRIPTION AND EXPERIMENTAL RESULTS FOR VAPOR MOTION IN ARBITRARY STRONG EVAPORATION

Tor YTREHUS

JUNE 1975

RHODE SAINT GENESE BELGIUM

von KARMAN INSTITUTE FOR FLUID DYNAMICS

TECHNICAL NOTE 112

KINETIC THEORY DESCRIPTION AND EXPERIMENTAL RESULTS FOR VAPOR MOTION IN ARBITRARY STRONG EVAPORATION

Tor YTREHUS

JUNE 1975

TABLE OF CONTENTS

ABSTRACT

The kinetics of the vapor motion due to arbitrary strong evaporation/condensation from an infinite, plane interphase boundary are studied using a moment method of the Mott-Smith, Liu-Lees type. Detailed calculations are performed for the case of net evaporation assuming a vapor of Maxwell molecules.

An equivalence is shown to exist between the vapor motion and the gas flow effusing from a perforated wall. Simple transformation rules are established so that experimental information on evaporation can be obtained from measurements performed in effusive flow fields.

The theoretical and experimental results are compared with existing analytical, numerical and Monte Carlo results.

LIST OF FIGURES

LIST OF SYMBOLS

a	force constant in molecular interaction law
$a_i(x)$	amplitude functions for modes in distribution function
b	collisional parameter
$\vec{c}$	$= \vec{\xi}-\vec{u}$: random molecular velocity
$\underline{dc}$	$= dc_x dc_y dc_z$: volume element in velocity space
f	molecular distribution function
g	$= \lvert\vec{\xi}-\vec{\xi}_1\rvert$: relative molecular velocity
k	Boltzmann constant
ℓ	kinetic scaling length (Eq. 52)
m	molecular mass
$\dot{m}$	number flux
m_L	$= n_L \sqrt{\frac{RT_L}{2\pi}}$: evaporated number flux
n	number density
n_e	$= qn_0$: effusion density
p	thermodynamic pressure
q	porosity factor
$\dot{q}_w$	heat flux (Eq. 63)
r	parameter in moment collision term (Eq. 48)
u_e	$= \sqrt{\frac{RT_0}{2\pi}}$: effusion velocity
u_L	$= \sqrt{\frac{RT_L}{2\pi}}$: evaporation velocity
u	bulk velocity
x	Cartesian coordinate
z	$= q\frac{p_0}{p_M}$: pressure-porosity parameter
z_L	$= \frac{p_L}{p_\infty}$: pressure parameter

$A_2(4)$	potential constant for Maxwell molecules
$B, B_{\mu\nu}$	kinetic transfer parameters
C	factor in moment collision term
$\tilde{F}^{\pm}$	
$\tilde{G}^{\pm}$	functions of downstream speed ratio
$\tilde{H}^{\pm}$	defined in Eqs. 17, 36
J	binary collision term
M_∞	$= \dfrac{u_\infty}{\sqrt{\gamma R T_\infty}}$: Mach number in downstream flow
R	$= \dfrac{k}{m}$: gas constant per unit mass
S_∞	$= \dfrac{u_\infty}{\sqrt{2RT_\infty}}$: speed ratio at downstream equilibrium
T	absolute temperature
α^-	$= \bar{a_4}(0)$: boundary value for BGK-mode
β^-	$= \bar{a_3}(0)$: boundary value for mode describing backscattering
γ	ratio between specific heats
$\gamma(z,x)$	incomplete gamma function
$\Gamma(z)$	complete gamma function
λ	molecular mean free path
μ	viscosity coefficient
$\vec{\xi}$	absolute molecular velocity
$\underline{d\xi}$	$= d\xi_x d\xi_y d\xi_z$: volume element in velocity space
σ	differential cross section
Σ	$= n_\infty u_\infty$: constant number flux at equilibrium
τ_{xx}	element of viscous stress tensor (Eq. 43)
ϕ_1, ϕ_2	functions in moment collision term (Eq. 47)
χ	deflection angle in two-body interaction
ψ_M	functions of molecular velocity

Subscripts

$()_1, ()_L$	evaporated mode
$()_3, ()_\infty$	downstream equilibrium mode
$()_i$	general basic mode
$()_w$	conditions at phase boundary

Superscripts

$()^+$	quantity related to $\xi_x > 0$ part of molecular velocity space
$()^-$	quantity related to $\xi_x < 0$ part of molecular velocity space

1. INTRODUCTION

The problem of vapor motion close to liquid-gas or solid-gas interphase boundaries has received considerable attention recently due to its increasing importance in various fields of engineering, including physics and vacuum technology. Applications are very diversified and include such areas as the sodium cooling of nuclear reactors, the extreme evaporation from metal surfaces exposed to high intensity laser radiation, space contamination problems and the problem of small, but often important, reactions on spacecrafts produced by the evaporation into empty space of material from adhesive joints or other components of the vehicle. The problem has also a certain interest to meteorology, because the growth and decay of water droplets are largely governed by the evaporation and condensation from the droplet surface. In addition, the problem of evaporation and condensation has intrinsic theoretical interest, because the description of the vapor motion must be based on kinetic theory for a general Knudsen layer in which all the gas dynamic variables: density, velocity and temperature undergo significant changes.

No analytical results covering a wide range of flow conditions seem to be available, due to well-known difficulties in solving non-linear kinetic equations, and even the case of weak evaporation into a background of the same gas is only partly adequately represented by the results that have been derived so far.

Some approximate results have been obtained by Hertz (Ref. 1) and Knudsen (Ref. 2) who computed the evaporated or condensed mass flux based on equilibrium considerations. The evaporation was represented by a half-range Maxwellian with parameters n_L and T_L, so that n_L would be the density corresponding to phase equilibrium at the temperature T_L, and the condensing mass flux was similarly computed from a downstream stationary Maxwellian with slightly different density and temperature

n_∞ and T_∞, respectively. In this way the so-called Hertz-Knudsen formula

$$\dot{m} = n_L \sqrt{\frac{RT_L}{2\pi}} \left(\frac{\Delta n}{n_L} + \frac{1}{2}\frac{\Delta T}{T_L}\right) \qquad (1)$$

$$(\Delta n \equiv n_L - n_\infty, \qquad \Delta T \equiv T_L - T_\infty)$$

for the net evaporated mass flux was derived. Generally, the change in temperature is neglected and the formula then reads

$$\dot{m} = (n_L - n_\infty) \sqrt{\frac{RT_L}{2\pi}} \qquad (2)$$

In either of the two versions above, the Hertz-Knudsen formula is found to underestimate the mass flux by a factor of 2, principally because the convective motion in the downstream vapor flow was neglected.

This fact was realized and correctd by Schrage (Ref. 3) and by Kucherov and Rikenglas (Ref. 4), who introduced a bulk velocity in the downstream Maxwellian when computing the flux of upstream directed vapor molecules. However, they neglected collisional effects in the Knudsen layer and, more importantly, they gave no way of relating the downstream bulk velocity to the known parameters in the problem. The Schrage formula (Section 6) therefore became empirical in nature, requiring measured values of the downstream vapor velocity. In addition, the fact that the quantities Δn and ΔT are coupled through the finite velocity flow field created in the vapor is missing in this approach.

The coupling between the downstream variables, and their correct relation to the conditions at the interphase boundary, can only be affected by the dynamic equations governing the vapor motion arbitrarily close to that boundary, and so must be an outcome of the Boltzmann equation, or of suitable approximations to that equation. Shankar and Marble (Ref. 5) derived

moment equations from the Boltzmann equation for the problem, using a Liu-Lees distribution function (Ref. 6), and considered the linearized,unsteady version of these equations. In the steady state limit they obtained mass fluxes that were rather close to the Hertz-Knudsen predictions. Patton and Springer (Ref. 7) on the other hand, obtained results that were twice the Hertz-Knudsen mass flux by a similar linearized analysis of the evaporation and condensation between two parallel plates.

In addition, there have been a number of papers dealing with the problem of weak evaporation into a background of a different gas where the kinetic corrections to the external macroscopic gradients can be computed from linearized Boltzmann or BGK-equations (Refs. 8, 9 and Refs. 10, 11, 12, respectively).

The limiting case of strong evaporation into vacuum has been treated by Anisimov (Ref. 13) and by Luikov et al. (Ref. 14) for a plane interface boundary, and by Edwards and Collins (Ref. 15) for a spherical interphase boundary with a radius that is large compared to a mean free path in the flow.

Numerical results for arbitrarily strong evaporation have been obtained by Kogan and Makasev (Ref. 16) who solved the non-linear BGK equation for the steady state problem, and by Murakami (Ref. 17) and by Murakami and Oshima (Ref. 18), who made Monte Carlo simulations of the transient vapor motion following a sudden change in the phase equilibrium at a variety of flow conditions. In addition, Yen (Refs. 19, 20) has obtained numerical solutions to the non-linear Boltzmann and BGK equations for the evaporation and condensation between two parallel plates, also at a wide range of non-equilibrium flow conditions.

The present study is intended to give a simple kinetic theory description of vapor motion for arbitrary strong evaporation- or condensation rates at the interphase boundary. Only steady state situations will be considered and only the case of net evaporation is treated in detail. A moment method that

combines the features of the Mott-Smith (Ref. 21) and the Liu-Lees (Ref. 6) methods is used along with the assumption that the vapor may be represented as an ideal gas of Maxwell molecules.

The important coupling between the gas dynamic variables in the downstream flow is described by the conservation equations, and it is shown that there is only one free driving parameter in the problem, for instance, the pressure parameter $z_L = p_L/p_\infty$. The other downstream quantities n_∞, u_∞ and T_∞ are unique functions of this parameter, and they are obtained by solving the non-linear conservation equations for the problem. The non-equilibrium contribution to the backscattering of molecules into the phase boundary and hence the net mass flux, is obtained from the same solution - also as a function of z_L.

Under conditions of weak, or moderately strong evaporation, the equations may be linearized and a simple, improved version of the Hertz-Knudsen formula is obtained, showing explicitly the effects of convective motion and non-equilibrium backscattering on the mass flux. The resulting mass flux is approximately twice the value predicted by the simple Hertz-Knudsen theory.

It is shown that the maximum value of the mass flux occurs at sonic downstream conditions, and that a steady state cannot exist at these conditions.This last result is not only an outcome of the non-linear collision term of the ξ_x^2-moment equation, but also the Boltzmann H-theorem is shown to be violated for steady state, supersonic flow conditions. The present analytical results are in good agreement with Kogan's (Ref. 16) numerical solution of the non-linear BGK equation and with Murakami's Monte Carlo simulation (Refs. 17,18), for the vapor motion in a similar physical system.

In the last section of this note we discuss a simple analogy with the related problem of molecular effusion from a perforated wall, for which theoretical and experimental results

have been previously obtained by the author (Refs.22,23,24,30). Simple transformation rules are established, whereby all the results from the effusion problem can be directly transformed into equivalent results for the kinetics of the vapor motion at arbitrarily strong evaporation rates.It is of particular interest to note that the transformation applies equally well to experimental and theoretical quantities, thus suggesting that experimental information on the vapor motion can be extracted from measurements in the physically simpler system of effusive flow. This has provided comparison of some of the theoretical results with experimental quantities, such as backscattered flux at the phase boundary and the speed ratio in the downstream equilibrium flow, over a wide range of conditions. Conclusions can therefore be drawn as to the validity of the present method, as well as other methods discussed in this note, in describing flows that are driven by arbitrary strong evaporation.

2. STEADY STATE EVAPORATION AND CONDENSATION PROBLEM

We consider the steady state limit of the following one dimensional time-dependent problem : a liquid (or solid) is initially in equilibrium with its pure vapor occupying the half space, $x \geq 0$, at the uniform temperature and pressure T_0 and p_0, respectively. At the time $t = 0$, the surface temperature of the condensed phase changes discontinuously to the value T_L and is kept constant at this value throughout the procedure. Then, evaporation or condensation begins through the phase boundary according to some specific relation among T_0, p_0, T_L and p_L, where p_L is the vapor saturation pressure at temperature T_L.

Let us further assume that, far downstream of the phase boundary, there is an idealized, flat sink or source for the vapor, that can instantaneously match the mass flow created. Then it is reasonable to assume that, after a time sufficiently long for transients to have died out or to have propagated through the system, a steady state will be accomplished in which the flow far from the phase boundary is a uniform equilibrium flow with constant parameters n_∞, u_∞ and T_∞ (Fig. 1). These are the downstream gas dynamic variables in the problem, with values depending upon the conditions at the phase boundary. A kinetic boundary layer will then form between the phase boundary and the downstream equilibrium region, in which non equilibrium effects may significantly influence the motion of the vapor. It is the kinetics of the vapor in this layer and in the asymptotic downstream state that will be pursued here; other phenomena related to the phase transition and to the condensed phase being left out of consideration.

The vapor molecules that are evaporated from the interphase surface are assumed to have a Maxwellian distribution in the velocity half-space $\xi_x > 0$, and we have therefore, in accordance with Eqs. 1 and 2, the usual description

$$f_L^+ = \frac{n_L}{(2\pi RT_L)^{3/2}} \exp\left(-\frac{\xi^2}{2RT_L}\right), \qquad \xi_x > 0 \quad \text{at } x = 0 \quad (3)$$

where n_L is the saturation density corresponding to T_L. It is further assumed that all impinging molecules are condensed into the phase boundary, and that reemission occurs through evaporation, only, which is equivalent to setting the absorption coefficient equal to unity.

It is reasonable to assume that the downstream pressure level, p_∞, can be controlled and we thus ask for the remaining downstream quantities - including the net evaporated mass flux - and the structure of the kinetic boundary layer for given values of n_L and T_L.

3. METHOD OF SOLUTION

The previous section defines the following problem for the one dimensional, steady state Boltzmann equation :

$$\xi_x \frac{\partial f}{\partial x} = \int_{\vec{\xi}_1} \int_{\chi} \int_{\varepsilon} (f'f_1' - ff_1)\, g\sigma(\chi, g) \sin\chi \, d\chi \, d\varepsilon \, \underline{d\xi_1} \qquad (4)$$

$$x = 0 : f = f_L^+ , \xi_x > 0 ; \quad x \to \infty : f \to f_\infty$$

where we have used standard notations in the collision term (Ref. 25), and where f_∞ is the downstream drifting Maxwellian, i.e.

$$f_\infty = \frac{n_\infty}{(2\pi RT_\infty)^{3/2}} \exp\left\{-\frac{(\xi_x - u_\infty)^2 + \xi_y^2 + \xi_z^2}{2RT_\infty}\right\} \qquad (5)$$

This equation is too complicated for a detailed analytical solution to be obtained, and we therefore resort to a simplified description where the Boltzmann equation is satisfied in some average sense, only, but such that the basic features of the non-linear collision term are preserved. The Mott-Smith moment method (Ref. 21), as previously applied to shock structure problem, is capable of doing this, but, because of the boundary condition at x = 0, the ansatz for the distribution function must contain half-range modes in velocity space, much in the same way as in the Liu-Lees method for Couette flow problems (Ref. 6). Here, however, the discontinuity in velocity space is with respect to the velocity component in the direction of bulk motion, and this makes the actual calculations somewhat more complicated than in either of the two original methods above.

The following trimodal ansatz is applied

$$f(x, \vec{\xi}) = a_1^+(x) f_L^+ + a_3^+(x) f_\infty^+ + a_3^-(x) f_\infty^- \qquad (6)$$

where the downstream Maxwellian has been split into the two half-range functions

$$f_\infty^+ = f_\infty, \ \xi_x > 0, \qquad f_\infty^- = f_\infty, \ \xi_x < 0 \tag{7}$$

The boundary conditions of Eq. 4 will be satisfied exactly, and this means in terms of the amplitude functions $a_i^{\pm}(x)$:

$$\begin{aligned} x = 0: \quad & a_1^+(0) = 1 \\ & a_3^+(0) = 0 \\ & a_3^-(0) = \beta^- \end{aligned} \qquad\qquad \begin{aligned} x = \infty: \quad & a_1^+(\infty) = 0 \\ & a_3^+(\infty) = a_3^-(\infty) = 1 \end{aligned} \tag{8}$$

where β^- is an unknown boundary parameter that must be obtained from the solution of the problem.

Moment equations are then derived from Eq. 4 in the standard way, i.e., by multiplying with functions ψ_μ of molecular velocity, and integrating over the entire velocity-space. Choosing for the first three ψ_μ 's the collisional invariants $1, \xi_x, \frac{1}{2}\xi^2$ and for the fourth one a non-conserved quantity ψ_4, we have

$$\begin{aligned} &\frac{\partial}{\partial x} \int \xi_x \psi_\mu \, f \, \underline{d\xi} = 0 \quad , \qquad \mu = 1, 2, 3 \\ &\frac{\partial}{\partial x} \int \xi_x \psi_4 \, f \, \underline{d\xi} = \int \psi_4 \, J(ff_1) \, \underline{d\xi} \end{aligned} \tag{9}$$

where we have written $J(ff_1)$ for the collision term in Eq. 4. The first three of these equations integrate to the usual conservation equations of one dimensional gas dynamics, whereas the last equation will yield a non-linear differential equation for the amplitude functions $a_i^{\pm}(x)$ when the interaction law for Maxwell molecules is inserted.

The number of moment equations required to determine the three amplitude functions $a_1^+(x)$, $a_3^{\pm}(x)$, is in principle only three, but it is clear that first of all the three conservation equations must be satisfied and that at least one further equation for a non-conserved quantity must be used, so that the total number of equations will be four. Only three of the equations are, however, linearly independent because of certain

conditions that are imposed on the coefficients of the system. by the conservation equations written for $x = 0$ and $x = \infty$, respectively (Section 5). This situation is similar to the shock structure problem where the compatibility conditions are the Rankine-Hugoniot equations relating the states of the two sides of the shock.

The present method of solution is identical to the method used in Refs. 22, 23 and 24 to treat the effusive flow problem, and also identical to the method used by Anisimov in Ref. 13 and by Liukov et al. in Ref. 14 in treating the limiting case of strong evaporation into vacuum. These last authors solved the conservation equations for one set of flow conditions (sonic), only, and estimated the thickness of the corresponding Knudsen layer from the BGK collision model. In this way, many of the interesting features of the solution were not noticed.

4. A GAS DYNAMIC CONNECTION PROBLEM

4.1 Relations between boundary and downstream conditions

Before asking for the structure of the vapor boundary layer, i.e., before attempting to solve the complete set of local transfer equations, Eqs. 9 of the previous section, for the amplitude functions $a_i(x)$, we must make use of the relations that these equations imply between the conditions at the phase boundary and at downstream equilibrium. These relations will, in fact, enable us to obtain the downstream parameters n_∞, u_∞ and T_∞, as well as the boundary parameter β^-, in terms of quantities that are controlled in the problem, and the states at the two sides of the Knudsen layer will therefore be known.

Let us write the integrated conservation equations at $x = 0$ and at $x = \infty$, respectively, to obtain

$$\left(\int \xi_x \, \psi_\mu \, f \, \underline{d\xi}\right)_{x=0} = \left(\int \xi_x \, \psi_\mu \, f \, \underline{d\xi}\right)_{x=\infty} \qquad \mu = 1,2,3 \qquad (10)$$

where the distribution function Eq. 6 with the boundary conditions Eq. 8 is to be inserted. More explicitly, this yields the present problem's counterparts to the Rankine-Hugoniot equations and may be written as follows (Appendix 1) :

$$n_L u_L - \beta^- n_\infty \sqrt{\frac{RT_\infty}{2\pi}} \, \tilde{F}^- = n_\infty u_\infty \qquad (11)$$

$$\frac{1}{2} n_L R T_L + \beta^- \frac{1}{2} n_\infty R T_\infty \tilde{G}^- = n_\infty u_\infty^2 + n_\infty R T_\infty \qquad (11)$$

$$2 n_L u_L R T_L - \beta^- 2 n_\infty R T_\infty \sqrt{\frac{RT_\infty}{2\pi}} \, \tilde{H}^- = n_\infty u_\infty \left(\frac{1}{2} u_\infty^2 + \frac{5}{2} R T_\infty\right)$$

where the velocity u_L is defined as

$$u_L = \sqrt{\frac{RT_L}{2\pi}} \qquad (12)$$

and where the functions $\tilde{F}^-$, $\tilde{G}^-$ and $\tilde{H}^-$ contain error functions, exponentials and powers of the downstream speed ratio $S_\infty = u_\infty/\sqrt{2RT_\infty}$ as given in Appendix 1. The system of equations expresses the fact that fluxes of mass, momentum and energy are the same at the phase boundary and at downstream equilibrium. The equations have been written for the case of net evaporation only, assuming u_∞ to be positive.

The equations may be restated in a more convenient, non dimensional form

$$z_L \sqrt{\frac{T_\infty}{T_L}} - \beta^- \tilde{F}^- = 2\sqrt{\pi}\, S_\infty$$

$$z_L + \beta^- \tilde{C}^- = 4S_\infty^2 + 2 \qquad (13)$$

$$z_L - \beta^- \sqrt{\frac{T_\infty}{T_L}}\, \tilde{H}^- = \sqrt{\frac{T_\infty}{T_L}}\, \sqrt{\pi}\, S_\infty \left(S_\infty^2 + \frac{5}{2}\right)$$

with z_L being a given driving parameter defined as the ratio between the saturation vapor pressure p_L and the background pressure p_∞, i.e.

$$z_L = \frac{p_L}{p_\infty} \qquad (14)$$

and with S_∞, $\sqrt{\frac{T_\infty}{T_L}}$ and β^- being the unknown quantities of the system. A solution may therefore be obtained for these quantities in terms of z_L, and the downstream state will then be completely specified because the density follows from the simple relation

$$\frac{n_\infty}{n_L} = \frac{1}{z_L \frac{T_\infty}{T_L}} \qquad (15)$$

This shows that only one of the downstream parameters, for instance the pressure p_∞, can be chosen freely, whereas the other parameters follow from the solution of the conservation equations. The coupling between the downstream parameters thus affected by the finite flow velocity u_∞, is equally important in the cases of strong and weak evaporation, which means that the quantities Δn and ΔT in formula (1) can never be treated as independent driving terms. This point was also realized by Shankar and Marble in Ref. 5.

It is furthermore realized that the physical properties of the vapor, i.e., the molecular interaction law, do not enter into this gas dynamic part of the problem.

4.2 Non-linear results

The solution of the previous system of normalized conservation equations, Eqs. 13, is straightforward in principle, but due to the non-linear character of the equations and to the complicated form of the functions $\tilde{F}^-$, $\tilde{G}^-$ and $\tilde{H}^-$, the resulting expressions become cumbersome in the general case, and the solution must be obtained numerically.

The speed ratio S_∞ appears to be the natural parameter in terms of which all the other quantities should be expressed. By eliminating the boundary parameter β^- and the temperature ratio $\sqrt{T_\infty/T_L}$ in Eqs. 13, the following relation between the driving parameter z_L and the speed ratio S_∞ is obtained :

$$z_L^2(\tilde{G}^{-2}-\tilde{F}^-\tilde{H}^-) + z_L\left\{2(4S_\infty^2+2)\tilde{F}^-\tilde{H}^- + 2\sqrt{\pi}\,S_\infty\,\tilde{G}^-\tilde{H}^- + \sqrt{\pi}\,S_\infty(S_\infty^2+\frac{5}{2})\,\tilde{F}^-\tilde{G}^-\right)$$

$$-\left((4S_\infty^2+2)^2\tilde{F}^-\tilde{H}^- + (4S_\infty^2+2)\sqrt{\pi}\,S_\infty(S_\infty^2+\frac{5}{2})\tilde{F}^-\tilde{G}^- + (4S_\infty^2+2)2\sqrt{\pi}\,S_\infty\tilde{G}^-\tilde{H}^-\right.$$

$$\left.+2\pi S_\infty^2(S_\infty^2+\frac{5}{2})\tilde{G}^{-2}\right) = 0 \qquad (16)$$

where $\tilde{F}^-$, $\tilde{G}^-$ and $\tilde{H}^-$ may be expressed as

$$\tilde{F}^- = -\sqrt{\pi}\, S_\infty \, \mathrm{erfc}S_\infty + e^{-S_\infty^2}$$

$$\tilde{G}^- = (2S_\infty^2+1)\mathrm{erc}S_\infty - \frac{2S_\infty}{\sqrt{\pi}}\, e^{-S_\infty^2}$$

$$\tilde{H}^- = -\frac{\sqrt{\pi}\, S_\infty}{2}\,(S_\infty^2+\frac{5}{2})\,\mathrm{erfc}S_\infty + \frac{1}{2}\,(S_\infty^2+2)\, e^{-S_\infty^2}$$

with $\mathrm{erfc}S_\infty$ being the complementary error function, i.e.,

$$\mathrm{erfc}S_\infty = 1 - \mathrm{erf}S_\infty = 1 - \frac{2}{\sqrt{\pi}} \int_0^{S_\infty} e^{-t^2}\, dt \qquad (18)$$

Although the coefficients of Eq. 16 are very complicated and contain some transcendental functions, the equation is essentially a second degree algebraic equation for the parameter z_L in terms of S_∞, and it can be solved numerically without any difficulties. Only one of the two roots is positive for positive values of S_∞, and that solution is contained in Table 1 and is furthermore shown plotted in Fig. 2a.

The remaining quantities now follow directly from Eqs. 13, i.e.,

$$\beta^- = \frac{4S_\infty^2+2-z_L}{\tilde{G}^-}$$

$$\sqrt{\frac{T_\infty}{T_L}} = \frac{z_L}{\beta^-\tilde{H}^- + \sqrt{\pi}\, S_\infty (S_\infty^2+\frac{5}{2})} \qquad (19)$$

and the density is given by the simple expression Eq. 15. The quantities are tabulated in Table 1 and plotted in Figs 2b,c,d. It is possible to demonstrate that, for values of S_∞ above approximately 0.6, the following asymptotic law applies for β^- :

$$\beta^- \sim e^{S_\infty^2} \qquad (20)$$

as indicated in Fig. 2d.

Now, β^- is the value of the amplitude function a_3^- for the distribution function f_∞^- at the phase boundary, and therefore is the amplitude of the distribution function describing molecules that are scattered back into the boundary. The value $\beta^- = 1$ corresponds to equilibrium and therefore to an abscence of Knudsen layer effects. On the other hand, $\beta^- > 1$ means that non-equilibrium backscattering occurs in the Knudsen layer, and more so the larger β^- is. At extreme conditions, that is when $S_\infty \gtrsim 0.6$, the non equilibrium backscattering is significant, tending to reduce the net evaporated number flux.

The number flux is expressed by the first of Eqs. 11, and the normalized version

$$\frac{\dot{m}}{\dot{m}_L} = \frac{1}{n_L \bar{u}_L} \left(n_L u_L - \beta^- n_\infty \sqrt{\frac{RT_\infty}{2\pi}}\, \tilde{F}^- \right) = \frac{n_\infty u_\infty}{n_L u_L} \qquad (21)$$

is contained in Table 1 and shown plotted versus the speed ratio S_∞ in Fig. 3. The function is practically flat above $S_\infty \gtrsim 0.6$ and it reaches a weak maximum (0.820) close to $S_\infty = 0.8$. This indicates that about 18% of the flux evaporated from the phase boundary is scattered back, mainly as a result of non-equilibrium collisions in the Knudsen layer close to the boundary, at extreme conditions of strong evaporation.

4.3 Linearized results. Improved Hertz-Knudsen formula

In the case of weak evaporation the downstream flow velocity u_∞ is small compared to the thermal velocity, i.e. $S_\infty << 1$, and the previous expressions may be linearized leading to simple and useful results.

To obtain the linearized version of the conservation equations, Eqs. 13, we first expand the functions $\tilde{F}^-$, $\tilde{G}^-$ and $\tilde{H}^-$ and have

$$\tilde{F}^- = 1 - \sqrt{\pi}\, S_\infty + O(S_\infty^2)$$

$$\tilde{G}^{-} = 1 - \frac{4}{\sqrt{\pi}} S_\infty + O(S_\infty^2) \qquad (22)$$

$$\tilde{H}^{-} = 1 - \frac{5}{4}\sqrt{\pi}\, S_\infty + O(S_\infty^2)$$

Then writing

$$z_L = 1 + \Delta z_L \quad , \quad \frac{T_\infty}{T_L} = 1 - \frac{\Delta T}{T_L}$$

$$\beta^{-} = 1 + \Delta\beta^{-} \qquad (23)$$

in Eq. 13, and neglecting products in small quantities, we obtain the linearized system

$$\Delta z_L - \frac{1}{2}\frac{\Delta T}{T_L} - \Delta\beta^{-} = 2\sqrt{\pi}\, S_\infty - \Delta\tilde{F}^{-}$$

$$\Delta z_L \qquad + \Delta\beta^{-} = \qquad \Delta\tilde{G}^{-} \qquad (24)$$

$$\Delta z_L + \frac{1}{2}\frac{\Delta T}{T_L} - \Delta\beta^{-} = \frac{5}{2}\sqrt{\pi}\, S_\infty - \Delta\tilde{H}^{-}$$

where we have also put $\tilde{F}^{-} = 1 - \Delta\tilde{F}^{-}$, etc. with

$$\Delta\tilde{F}^{-} = \sqrt{\pi}\, S_\infty, \qquad \Delta\tilde{G}^{-} = \frac{4}{\sqrt{\pi}} S_\infty \ , \qquad \Delta\tilde{H}^{-} = \frac{5}{4}\sqrt{\pi}\, S_\infty \qquad (25)$$

From the first of Eqs. 24 above it is clear that neglect of the downstream convective velocity when computing the mass flux, would imply neglect of the quantity $\Delta\tilde{F}^{-} = \sqrt{\pi}\, S_\infty$ in comparison with $2\sqrt{\pi}\, S_\infty$, and thus will never be justified, irrespective of the smallness of S_∞, and of u_∞.

The solution of the above system in terms of S_∞ is

$$\Delta z_L = \left(\frac{2}{\sqrt{\pi}} + \frac{9\sqrt{\pi}}{16}\right) S_\infty \ , \qquad \frac{\Delta T}{T_L} = \frac{\sqrt{\pi}}{4} S_\infty$$

$$\Delta\beta^{-} = \left(\frac{2}{\sqrt{\pi}} - \frac{9\sqrt{\pi}}{16}\right) S_\infty \qquad (26)$$

with a similar result for the density, i.e.

$$\frac{n_\infty}{n_L} = 1 - \frac{\Delta n}{n_L} = 1 - \left(\frac{2}{\sqrt{\pi}} + \frac{5\sqrt{\pi}}{16}\right) S_\infty \qquad (27)$$

The results are indicated with the straight lines on Figs 2a-d, and the linear approximation to $\tilde{F}^-$ is also shown in Fig. 2e. Only the temperature is reasonably well approximated by the linear result outside of the range of small S_∞ values.

A linearized expression for the number flux is now available, and we have

$$\dot{m} = n_L \sqrt{\frac{RT_L}{2\pi}} \left(\underbrace{\frac{\Delta n}{n_L} + \frac{1}{2}\frac{\Delta T}{T_L}}_{\sqrt{\pi}\, S_\infty} - \underbrace{\Delta\beta^-}_{0.1314 S_\infty} + \underbrace{\tilde{\Delta F}^-}_{\sqrt{\pi}\, S_\infty} \right) \qquad (28)$$

showing the relative importance of the various contributions

(i) Hertz-Knudsen theory $\left(\frac{\Delta n}{n_L} + \frac{1}{2}\frac{\Delta T}{T_L}\right)$

(ii) non-equilibrium backscattering $(\Delta\beta^-)$

(iii) downstream convective motion $(\tilde{\Delta F}^-)$

The non equilibrium backscattering is thus seen to be very moderate under conditions of weak evaporation, whereas the effect of convective motion is not.

Making use of Eq. 27 and of the simple fact that the sum in the above parenthesis equals $2\sqrt{\pi}\, S_\infty$, the expression for the number flux may be written

$$\dot{m} = (n_L - n_\infty) \sqrt{\frac{RT_L}{2\pi}} \frac{32\pi}{32+5\pi} \qquad (29)$$

where the value of the numerical factor is 2.107. This improved Hertz-Knudsen formula predicts a mass flux that is more than

twice the value given by the original version, Eq. 2.

Because the changes in density, temperature and pressure are uniquely related via the flow velocity u_∞, (Eqs. 26, 37) the result may also be given in terms of pressure drop, $\Delta p = p_L - p_\infty$, and we have

$$\dot{m} = n_L \sqrt{\frac{RT_L}{2\pi}} \frac{\Delta p}{p_L} \cdot \frac{32\pi}{32+9\pi} \qquad (30)$$

with the value of the numerical factor now being 1.668.

4.4 Limiting conditions. Boltzmann H-theorem

The question of what limiting steady state conditions can be reached downstream of the Knudsen layer in the case of strong evaporation, is not a trivial one, and must be settled by arguments from kinetic theory. In the conservation equations Eqs. 11, there is in fact nothing that prevents us from considering arbitrarily large supersonic downstream flow velocities for sufficiently large values of the pressure ratio p_L/p_∞. In complete analogy with the corresponding problem for the perforated wall effusion, we now demonstrate that the Boltzmann H-theorem implies that the speed ratio S_∞ must always be less than a certain value, corresponding to weakly supersonic flow. It will be shown later (Section 5.3) that the limit is even more restrictive, and that only subsonic flow conditions are actually possible.

The H-theorem for a bounded system under steady state conditions is (Refs. 26, 27)

$$\int_S dS \int_{\vec{\xi}} (\vec{\nu}\cdot\vec{\xi})\, f \ln f \, d\vec{\xi} \leq 0 \qquad (31)$$

where the integrals must be evaluated at the boundary S, having local outward directed normal $\vec{\nu}$. In the present case, this gives the inequality

$$\left(\int_{\vec{\xi}} \xi_x \, f \, \ell n f \, \underline{d\xi}\right)_{x=0} - \left(\int_{\xi} \xi_x \, f \, \ell n f \, \underline{d\xi}\right)_{x=\infty} \geq 0 \qquad (32)$$

where the distribution function must be taken in accordance with the boundary conditions and the solution obtained for $f^-\big|_{x=0}$, i.e.

$$x = 0 : f = \begin{cases} f_L^+ , & \xi_x > 0 \\ \beta^- f_\infty^- , & \xi_x < 0 \end{cases} \qquad x = \infty : f = f_\infty \qquad (33)$$

When the indicated integrations in the velocity space are carried out, using the results of Appendix 1, and the conservation equation for mass flux is used, the inequality (32) may be rewritten in explicit terms as

$$\ell n \frac{n_L}{n_\infty} \left(\frac{T_\infty}{T_L}\right)^{3/2} + \beta^- \frac{n_\infty}{n_L} \sqrt{\frac{T_\infty}{T_L}} \left[-F^- \ell n \beta^- + 2e^{-S_\infty^2} - \frac{3\sqrt{\pi}}{2} S_\infty (1 - \mathrm{erf} S_\infty)\right]$$

$$+ 3 \frac{n_\infty}{n_L} \sqrt{\frac{T_\infty}{T_L}} \sqrt{\pi} \, S_\infty - 2 \geq 0 \qquad (34)$$

The left-hand side of this inequality has been tabulated along with the gas dynamic parameters in Table 1 and is listed under the heading BF. This quantity is seen to be positive for values of S_∞ that are below 1.20, and the H-theorem is therefore satisfied up to this point, only. A graph of this function (BF) is given in Fig. 4 where the speed ratio S_∞ has been chosen as abscissa. Highly supersonic vapor velocities are thus seen to be impossible in the steady state limit in the process considered.

5. STRUCTURE OF THE VAPOR KNUDSEN LAYER

5.1 Local conservation equations

To compute the transition from the state at the phase boundary through the kinetic boundary layer to the state at downstream equilibrium, local conservation equations must be written and solved together with a transfer equation for a non-conserved quantity. The local conservation equations are as follows (Appendix 1) :

$$n_L u_L\, a_1^+(x) + n_\infty \sqrt{\frac{RT_\infty}{2\pi}}\, \tilde{F}^+ a_3^+(x) - n_\infty \sqrt{\frac{RT_\infty}{2\pi}}\, \tilde{F}^- a_3^-(x) = n_\infty u_\infty$$

$$\frac{1}{2} n_L RT_L\, a_1^+(x) + \frac{1}{2} n_\infty RT_\infty \tilde{G}^+ a_3^+(x) + \frac{1}{2} n_\infty RT_\infty \tilde{G}^- a_3^-(x) = n_\infty u_\infty^2 + n_\infty RT_\infty$$

$$2n_L u_L RT_L\, a_1^+(x) + 2n_\infty RT_\infty \sqrt{\frac{RT_\infty}{2\pi}}\, \tilde{H}^+ a_3^+(x) - 2n_\infty RT_\infty \sqrt{\frac{RT_\infty}{2\pi}}\, \tilde{H}^- a_3^-(x)$$

$$= n_\infty u_\infty \left(\frac{1}{2} u_\infty^2 + \frac{5}{2} RT_\infty\right) \qquad (35)$$

with $\tilde{F}^+$, $\tilde{G}^+$ and $\tilde{H}^+$ being the results of half-range integrations in the $\xi_x > 0$ part of the velocity space, and being related to previous functions from $\xi_x < 0$ integrations by

$$\tilde{F}^+ - \tilde{F}^- = 2\sqrt{\pi}\, S_\infty$$

$$\tilde{G}^+ + \tilde{G}^- = 4S_\infty^2 + 2$$

$$\tilde{H}^+ - \tilde{H}^- = \sqrt{\pi}\, S_\infty^3 + \frac{5}{2}\sqrt{\pi}\, S_\infty \qquad (36)$$

The equations may be exploi ed more easily in the non-dimensional version

$$z_L \sqrt{\frac{T_\infty}{T_L}}\, a_1^+(x) + \tilde{F}^+ a_3^+(x) - \tilde{F}^- a_3^-(x) = 2\sqrt{\pi}\, S_\infty$$

$$z_L\, a_1^+(x) + \tilde{G}^+\, a_3^+(x) + \tilde{G}^-\, a_3^-(x) = 4S_\infty^2 + 2$$

$$z_L\, a_1^+(x) + \sqrt{\frac{T_\infty}{T_L}}\, \tilde{H}^+ a_3^+(x) - \sqrt{\frac{T_\infty}{T_L}}\, \tilde{H}^- a_3^-(x) = \sqrt{\frac{T_\infty}{T_L}}\, \sqrt{\pi}\, S_\infty (S_\infty^2 + \frac{5}{2}) \qquad (37)$$

It is easy to show that, with the Rankine-Hugoniot like relations Eqs. 11 or Eqs. 13 being satisfied by z_L, S_∞ and T_∞/T_L, the above system of three linear equations for the three amplitude functions a_1^+, a_3^+ and a_3^- is singular and therefore does not specify a non-trivial solution for these quantities. If this was not so, the structure of the kinetic boundary layer would follow from the conservation equations alone, without any collisional effects being involved, thus leading to highly contradictory results. The Rankine-Hugoniot like equations in the gas dynamic problem are therefore necessary conditions for a solution of the full kinetic problem to exist, in complete analogy with the Mott-Smith approach for the shock structure problem.

Only two of the three equations (37) are thus linearly independent and the system therefore serves to express two amplitude functions in terms of the third one. By simple manipulations we find

$$a_1^+(x) = \frac{a_3^-(x) - 1}{\beta^- - 1}$$

$$a_3^+(x) = \frac{\beta^- - a_3^-(x)}{\beta^- - 1} \qquad (38)$$

which also means that a very simple relation exists between these two functions, namely

$$a_1^+(x) + a_3^+(x) = 1 \qquad (39)$$

Further progress must be based upon specific information on collisional effects, and for this we require a moment equation for a non-conserved quantity.

5.2 Transfer equation for $\psi_4 = \xi_x^2$

A natural choice for the non-conserved quantity is to take $\psi_4 = \xi_x^2$ in Eq. 9 and then use existing formulas for the resulting collision term for the case of Maxwell molecules ($F \sim \frac{1}{r^5}$). For that particular interaction law the cross section $\sigma(\chi,g)$ in the two-particle problem becomes inversely proportional to the relative velocity g, so that the product $\sigma \cdot g$ in Eq. 4 becomes a function of the deflection angle χ, only (Ref. 25). This considerably simplifies the evaluation of the collision term in any non-conserved moment equation, and in particular the collision operator does not create moments of higher order than those given by the function ψ_4 itself, i.e., $\int \psi_4 f \, \underline{d\xi}$ (Ref. 25).

By well-known results from the symmetry properties of the binary collision term (Ref. 25) we have in the general case

$$\int_{\vec{\xi}} \psi_4(\xi)\, J(ff_1)\, \underline{d\xi} = \int_{\vec{\xi}} \int_{\vec{\xi}_1} \int_{\chi} \int_{\varepsilon} \psi_4(\xi)(f'f_1' - ff_1) g\sigma(\chi,g) \sin\chi \, d\chi \, d\varepsilon \, \underline{d\xi_1} \, \underline{d\xi}$$

$$= \int_{\vec{\xi}} \int_{\vec{\xi}_1} \int_{\chi} \int_{\varepsilon} \left(\psi_4(\vec{\xi}') - \psi_4(\vec{\xi})\right) ff_1 g\sigma(\chi,g) \sin\chi \, d\chi \, d\varepsilon \, \underline{d\xi_1} \, \underline{d\xi} \qquad (40)$$

where $\vec{\xi}'$ is related to $\vec{\xi}$ by the dynamics of a binary encounter. Because of the simplifications for Maxwell molecules noted above the ξ_1 and the χ-integrations can be performed independently and simple expressions will result from both integrations.

For $\psi_4 = \xi_x^2$ we have (Ref. 25, pp 364)

$$\int_{\vec{\xi}} \psi_4 J(ff_1)\, \underline{d\xi} = \frac{\pi}{\lambda_r m} \sqrt{\frac{RT_r}{2\pi}} \frac{n}{n_r} \tau'_{xx} \qquad (41)$$

where the mean free path λ_r in the reference state denoted by subscript "r" is related to the potential constants A (4) and a, or to the viscosity coefficient μ_r of the gas, by

$$\lambda_r = \frac{5}{16A_2(4)} \frac{1}{n_r} \sqrt{\frac{kT_r}{a}} \frac{1}{\Gamma(\frac{7}{2})} = \frac{\mu_r}{mn_r} \sqrt{\frac{\pi}{2RT_r}} \tag{42}$$

τ'_{xx} is the viscous part of the normal stress in the x-direction as obtained from the standard definition

$$\tau'_{xx} = - m \left(\int (\xi_x - u)^2 \, f \, \underline{d\xi} - \frac{1}{3} \int (\vec{\xi} - \vec{u})^2 \, f \, \underline{d\xi} \right) \tag{43}$$

where $\vec{u} = (u,0,0)$ is the local bulk velocity in the present one dimensional flow.

Also, by definition we have

$$n = \int f \, \underline{d\xi} \tag{44}$$

$$u = \frac{1}{n} \int \xi_x \, f \, \underline{d\xi}$$

so that the resulting moment equation for ξ_x^2

$$\frac{\partial}{\partial x} \int \xi_x^3 \, f \, \underline{d\xi} = \int \xi_x^2 \, J(ff_1) \, \underline{d\xi} \tag{45}$$

is non-linear in the moments of f occurring in the right hand side.

This equation must be worked out in terms of the basic amplitude functions, $a_i^{\pm}(x)$, after the expression for f_j

$$f(\vec{\xi},x) = a_1^+(x) f_L^+ + a_3^+(x) f_\infty^+ + a_3^-(x) f_\infty^-$$

has been inserted. Then the Eqs. 38 can be used to transform the result into a differential equation for one single amplitude function, only and a solution may be obtained. This procedure is reviewed in some detail in Appendix 2, from which we quote the following results

$$\int \xi_x^2 \, J(ff_1) \, \underline{d\xi} = \frac{\pi}{\lambda_L m} \sqrt{\frac{RT_L}{2\pi}} \, \frac{\frac{2}{3} m\Sigma^2}{8 n_L S_\infty^2} \, \phi_1 \phi_2 (\bar{a_3}-1)(\bar{a_3}-r) \qquad (46)$$

with $\Sigma \equiv n_\infty u_\infty$, and ϕ_1 and ϕ_2 being given as

$$\phi_1 = \frac{1}{\bar{\beta}-1} \left(\frac{n_L}{n_\infty} - 2 + \bar{\beta}(1-\mathrm{erf} S_\infty) \right)$$

$$\phi_2 = \frac{1}{\bar{\beta}-1} \left(z_L - 2 + \bar{\beta}(1-\mathrm{erf} S_\infty) \right) \qquad (47)$$

The parameter r is expressed as

$$r = 1 - \frac{2}{\phi_1} + \frac{4S_\infty^2}{\phi_2} \qquad (48)$$

and all these quantities are unique functions of the driving parameter z_L by the gas dynamic relations between the states at the phase boundary and at downstream equilibrium.

The convective term may similarly be expressed in terms of $\bar{a_3}$ alone, and the result is (Appendix 2)

$$\frac{\partial}{\partial x} \int \xi_x^3 \, f \, \underline{d\xi} = - \frac{2 n_L u_L R T_L}{\bar{\beta}-1} \left(1 - \frac{T_\infty}{T_L}\right) \frac{d\bar{a_3}}{dx} \qquad (49)$$

The moment equation (45) may therefore be written as

$$-B \frac{d\bar{a_3}}{dx} = \frac{C}{\lambda_L} (\bar{a_3}-1)(\bar{a_3}-r) \qquad (50)$$

where B, C and r are non zero, positive parameters that depend upon the flow conditions as indicated by the expressions above.

Therefore, if $r < 1$

the above equation describes a relaxation towards the correct downstream equilibrium $\bar{a_3} = 1$, so that both boundary conditions

on a_3^- from Eq. 8 are satisfied, i.e.,

$$a_3^-(0) = \beta^-, \quad (\beta^- > 1), \qquad a_3^-(\infty) = 1$$

Then the solution of Eq. 50 above is

$$\frac{a_3^-(x)-1}{a_3^-(x)-r} = \left(\frac{\beta^- -1}{\beta^- -r}\right) e^{-\frac{C}{B}\frac{(1-r)}{\lambda_L}x} \tag{51}$$

from which a proper scale for the thickness of the Knudsen layer appears to be

$$\ell = \frac{\lambda_L}{\frac{C}{B}(1-r)} \tag{52}$$

With one amplitude function being known, the other two follow from Eqs. 38, and the distribution function is therefore completely determined, revealing the corresponding structure of the Knudsen layer.

5.3 Properties of the solution

To discuss the solution for the amplitude functions found above, we first need to consider the actual values of the parameters B, C and r at all possible flow conditions. This is done in Table 2 where these quantites are tabulated as functions of the speed ratio, S_∞. It is seen that the ratio $\frac{C}{B}$ is of order unity at ordinary flow conditions, decreasing with increasing values of S_∞, and that the parameter r stays below unity for values of S_∞ below approximately 0.91 (Fig. 5). The product $\frac{C}{B}(1-r)$, which is also of order unity at intermediate conditions, therefore decreases strongly with S_∞ and becomes zero at the above critical value of S_∞ that makes r equal to one. The quantitative behaviour is shown in Fig. 6, where the reciprocal length Eq. 52 has been plotted versus the speed ratio S_∞.

In the range where we have

$$\frac{\lambda_L}{\ell} \equiv \frac{C}{B}(1-r) \sim O(1), \qquad \text{i.e. } S_\infty \lesssim 0.3$$

the solution Eq. 51 describes spatial relaxation through a Knudsen layer of thickness as the mean free path λ_L. At the higher values of S_∞, and in particular as we approach the critical value close to 0.91 [1], the thickness of the Knudsen layer increases strongly and finally becomes infinite.

In the limit r = 1 the differential equation (50) does, however; degenerate into the simpler version

$$-B \frac{da_3^-}{dx} = \frac{C}{\lambda_L}(a_3^- - 1)^2 \tag{53}$$

whose solution is given by

$$\frac{a_3^-(x)-1}{\beta^- - 1} = \frac{1}{1 + \frac{C}{B}(\beta^- - 1)\frac{x}{\lambda_L}} \tag{54}$$

This non-exponential solution implies a very slow approach towards downstream equilibrium, and evaluating the parameters entering, we have

$$\frac{C}{B}(\beta^- - 1) \simeq 0.05 \qquad (\text{at } r = 1,\ S_\infty \simeq 0.91)$$

so that a length scale

$$\ell = \frac{\lambda_L}{\frac{C}{B}(\beta^- - 1)} \tag{55}$$

is of the order of $20\lambda_L$. In order to complete 90% of the transition to the downstream sonic state, i.e., in order for $a_3^-(x)$ to reach the value 0.9, a value of x equivalent to some 250 mean free paths λ_L is therefore required, and this means that the

---

[1] The actual critical value is found to be 0.907.

downstream equilibrium is practically unattainable under these conditions.

At values of S_∞ greater than sonic, which are predicted by the conservation equations to occur for values of z_L above 4.8, we find

$$1 < r < \beta^-$$

and Eq. 50 has a solution that approaches the downstream value $a_3^- = r$, rather than the equilibrium value $a_3^- = 1$. The downstream state corresponding to $a_3^- = r$ is clearly incompatible with the Rankine-Hugoniot-like conditions (11), and $a_3^- = r$ therefore represents a spurious equilibirum without any significance for the present problem.

The non-conserved moment equation (50) thus implies a relaxation towards a Maxwellian state only as long as the pressure ratio p_L/p_∞ is below 4.8 and the flow is subosnic. This results is a little more restrictive than the limit $S_\infty \leq 1.2$ which was derived from the Boltzmann H-theorem.

At low evaporation rates, corresponding to small deviations from equilibrium, $f_L^+ = f_\infty^+$, Eq. 50 may be linearized with the substitution

$$a_3^-(x) = 1 + h(x) , \qquad |h(x)| \leq \Delta\beta^- \tag{56}$$

We thus get

$$-\frac{dh}{dx} = \frac{C}{B}\frac{(1-r)}{\lambda_L} h$$

$$h(0) = \Delta\beta^- \tag{57}$$

where the coefficient $\frac{C}{B}(1-r)$ may be evaluated from linearized expressions for $S_\infty << 1$, and $\Delta\beta^-$ is the linearized boundary value given in Eq. 26.

It is readily verified that

$$\frac{C}{B}(1-r) = \frac{4}{3}, \qquad (S_\infty << 1) \tag{58}$$

so that the solution for h(x) is

$$h(x) = \Delta\beta^- \, e^{-x/\frac{3}{4}\lambda_L} \tag{59}$$

We therefore have

$$a_3^-(x) = 1 + \Delta\beta^- \, e^{-x/\frac{3}{4}\lambda_L}$$

$$a_1^+(x) = \frac{h(x)}{\Delta\beta^-} = e^{-x/\frac{3}{4}\lambda_L} \tag{60}$$

$$a_3^+(x) = 1 - \frac{h(x)}{\Delta\beta^-} = 1 - e^{-x/\frac{3}{4}\lambda_L}$$

and the scaling length for the Knudsne layer thickness is $\frac{3}{4}\lambda_L$.

5.4 Discussion

Some results revealing the structure of the Knudsen layer at arbitrarily strong evaporation rates are shown in Figs. 6-10.

From Fig. 6 the thickening of the Knudsen layer with increasing S_∞, which means increasing evaporation rates, is apparent. According to the present solution, the sonic state can never be achieved with the downstream flow being close to equilibrium. Two interpretations of this result are possible : either the flow must become unsteady in the sonic limit, or, there are not enough collisions to affect a downstream equilibrium when the pressure ratio $z_L = p_L/p_\infty$ exceeds the critical value close to 4.8. In the latter case a very complicated transition from a Knudsen layer type of flow close to the boundary

into a non-equilibrium rarefaction wave extending to infinity will occur.

Figures 7, 8, 9 and 10 show the relaxation of the basic modes in the distribution function and of the macroscopic quantities density, velocity and temperature at typical flow conditions; S_∞ : 0.3, 0.5, 0.7. The vapor is seen to expand, almost isothermally, away from the phase boundary, after a rather pronounced microscopic jump in temperature has been taking place at the boundary. For the typical flow conditions of $S_\infty = 0.5$ we quote the numbers

$$\frac{T(0)}{T_L} = 0.85, \qquad \frac{T_\infty}{T_L} = 0.80$$

which means that 75 per cent of the total drop in temperature, from the evaporation temperature T_L at the interphase to the equilibrium temperature T_∞ far downstream, is affected by the microscopic jump at the boundary. This percentage is slightly less at higher evaporation rates, and larger at lower evaporation rates - and downstream flow velocities.

The macroscopic quantities were obtained from the standard definitions

$$n = \int f \, \underline{d\xi} \quad , \qquad \frac{3}{2} nkT = \int \frac{1}{2} m c^2 f \, \underline{dc}$$

resulting in the explicit formulas

$$\frac{n}{n_\infty} = \left(\bar{a_3}(x)-1\right) \frac{1}{2} \phi_1 + 1 \tag{61}$$

$$\frac{T}{T_\infty} = \frac{1}{3} \frac{n_\infty}{n} \left[2S_\infty^2+3+\left(\bar{a_3}(x)-1\right)\phi_2-2S_\infty^2 \frac{n_\infty}{n} \right]$$

with ϕ_1 and ϕ_2 being defined in the previous Eqs. 47, and with $\bar{a_3}(x)$ being given by the solution (51). The spatial relaxation is contained in one mode only, such as $\exp(-\frac{x}{\ell})$ which is a result of the fact that only one non-conserved moment equation has been used to describe the structure of the flow.

6. COMPARISON WITH EXISTING RESULTS

6.1 Linearized results

For the case of weak evaporation or condensation, several theoretical papers present both approximate and exact results based upon the linearized Boltzmann or BGK equation, or based upon linearized solutions to systems of moment equations.

Pao (Ref. 10) derived the following approximate results from the linearized BGK equation

$$\frac{\Delta T}{T_L} = \frac{\sqrt{\pi}}{4} S_\infty , \qquad \frac{\Delta n}{n_L} = \frac{7\sqrt{\pi}}{8} S_\infty \tag{62}$$

$$\dot{m} = 2n_L \sqrt{\frac{RT_L}{2\pi}} \left[\frac{\Delta n}{n_L} + \frac{1}{2} \frac{\Delta T}{T_L}\right]$$

which are very close to our linearized results, Eqs. 26-29. In fact, the temperature change is exactly the same, and the density change and the mass flux are only slightly smaller, by 8 and 5 per cent, respectively. The above results have been confirmed by Pao (Ref. 11) by an exact evaluation from the linearized BGK equations, and by Loyalka (Ref. 8) and Cipolla et al. (Ref. 9) who considered the linearized Boltzmann equation for Maxwell molecules.

In addition, Patton and Springer (Ref. 7) have obtained evaporation rates that are twice the Hertz-Knudsen value for evaporation - condensation between two parallel plates by solving linearized moment equations derived by Liu-Lees' method.

Shankar and Marble (Ref. 5) on the other hand, obtained in a similar analysis for the half-space problem, results that are rather close to the Hertz-Knudsen values. They did, however, neglect the bulk velocity in the downstream Maxwellian and this will always lead to Hertz-Knudsen results. The authors emphasized the fact that only one of the downstream variables can be chosen freely in the problem and that therefore there is

only one free driving parameter, such as Δp, in Eq. 30.

6.2 Non-linear results

The non-linear formulation of the problem most often requires numerical evaluation, but a few approximate analytical results are available.

Anisimov (Ref. 13) and Luikov et al. (Ref. 14) used the same Mott-Smith method as in the present study to compute the limiting case of strong evaporation from a plane metal surface into vacuum. Their calculation is therefore only for sonic downstream conditions, and the values obtained at this point are identical to the limiting values of the present analysis, Figs. 11, 12, 13. In particular they found $(m/m_L)_{cr} = 0.815$ which means that the backscattered flux is 18.5 percent of the evaporated flux at extreme conditions. Practically the same result has been obtained by Edwards and Collins (Ref. 15) for the approximate calculation of evaporation from a spherical drop into vacuum, using Grad's expression for the distribution function at the surface of the droplet. The structure of the Knudsen layer was estimated from the BGK collision term in Ref.14, and from the Navier-Stokes equations matched to a Grad-type of distribution function at the phase boundary in Ref. 15, and none of the treatments present any irregular behaviour at, or close to the sonic point. In fact, the analysis in Ref. 15 assumes that the sonic state, $M_\infty = 1$, can be reached by the vapor after expanding through a finite thickness Knudsen layer, which seems to be contradicted by the present results.

Kogan and Makashev (Ref. 16) solved the non-linear BGK equation numerically for the half-space evaporation problem, and obtained results as shown on Figs. 11 and 12. The agreement with the present results is good, except at extreme conditions, for which the accuracy of Kogan's numerical results are known to be poor (Ref. 28). For the heat flux from the phase boundary which is defined as

$$\dot{q}_w = \frac{1}{2} m \int_{\vec{\xi}} \xi_x \xi^2 \, f(0,\vec{\xi}) \, d\xi \qquad (63)$$

the agreement is substantial at all flow conditions (Fig. 12). The abscissa in Figs. 11, 12 is the number flux at the phase boundary normalized by the flux $n_L c_{m_L} = n_L \sqrt{2RT_L}$.

Yen (Refs. 19, 20) obtained numerical solutions of the discretized Boltzmann and BGK equations for evaporation-condensation between parallel plates. His results show the same qualitative trend as the present results, namely, that the non-equilibrium collisional effects tend to reduce the evaporation rate as compared to linear theory.

6.3 Monte-Carlo results

Murakami (Refs. 17,18) has made a Monte-Carlo simulation of the full unsteady version of the present half-space problem, and asymptotic steady state results are shown in Figs. 11, 12, 13. The parameter α is the condensation coefficient (taken to be unity in the present study) and the parameter β' [1] is defined as

$$\beta = \frac{\frac{(n_L - n_0)}{n_0}}{\frac{(T_L - T_0)}{T_0}} \qquad (64)$$

in terms of the notions explained in Section 2.

The agreement between the Monte Carlo results and the present calculations is very good for all quantities throughout the whole range of flow conditions considered. The non-linear deviation in mass flux at strong and moderately strong evaporation is evident (Fig. 11) and the almost flat maximum for S_∞ larger than 0.6 is apparent from both sets of

[1] Not to be confused with β^- in the present treatment.

results (Fig. 12). A maximum value in the number flux close to $0.85\ n_L\sqrt{RT_L/2\pi}$ may be inferred from the Monte Carlo results, and this is only slightly higher than the Mott Smith value, $0.82\ n_L\sqrt{RT_L/2\pi}$. Very few values for the heat flux are available from the Monte Carlo calculations and those at extreme conditions appear somewhat overestimated compared to the present and to Kogan's results.

Further substantial agreement is observed in the comparison of macroscopic jumps in density and temperature from the Monte Carlo and the present results (Fig. 13). The deviation in density jump from linear predictions in the Knudsen layer is of importance even for moderately strong evaporation. The temperature jump is on the other hand predicted quite accurately by the linear theory throughout the whole range of flow conditions [1].

The Monte Carlo results for the local structure of the evaporation Knudsen layer are also in qualitative agreement with the predictions from the present theory, and they show in particular that a steady downstream state is never accomplished at, or beyond Mach number equal to one. In those cases the Knudsen layer and thereby the non-equilibrium effects, are found to merge far into the downstream flow field through a kind of (non-equilibrium rarefaction wave (Ref. 18) and it is not clear if the ultimate downstream state will be exactly sonic, or not. Some results obtained with the Schrage formula, i.e. with $\beta^- = 1$ in the expression (11) :

$$\dot{m} = n_L u_L - n_\infty \sqrt{\frac{RT_\infty}{2\pi}}\ \tilde{F}^-\ (S_\infty)$$

---

[1] Observe that the odd trend in the Monte Carlo predicted temperatures at low evaporation rates is due to statistical scattering in that method.

are also shown in Fig. 11. The values for S_∞ were inferred from the Monte Carlo results in that figure. In addition to being incomplete from the theoretical point of view, the Schrage formula overestimates the mass flux at extreme conditions, due to neglect of non-equilibrium contributions to the backscattering. The present expression for the mass flux with $\beta^- \neq 1$ where S_∞ is a given function of $z_L = p_L/p_\infty$ is to be preferred due to consistent and easy application, and also due to improved accuracy at extreme conditions of high evaporation rates.

6.4 Experimental results

The only experimental results, on strong evaporation at least, that appear to be referred to in the literature, are those of Golubtsov (Ref. 29) for evaporation of tantalum into vacuum. They are shown in Fig. 11 and indicate mass fluxes close to the predicted upper limit. The downstream variables were, however, not obtained by measurements in the flow field itself, they were rather inferred from ambient pressure measurements in the background and accordingly these quantities are not well defined. In at least part of the experiments, the flow conditions were far from being one dimensional and this makes the assignment of any value n_∞ in Fig. 11 rather questionable.

In the following section we indicate a way of obtaining additional and more detailed experimental information by making use of an analogy between evaporation and the physically simpler situation of effusion from a perforated wall.

7. THE ANALOGY BETWEEN EVAPORATION AND PERFORATED WALL EFFUSION

7.1 Physical similarity

The problem of molecular effusion from a thin, perforated wall has been studied theoretically and experimentally in Refs. 22, 23, 24 and a complete report on the results is given in Ref. 30. The system is represented schematically and compared with the system used to represent evaporation in Fig. 14.

Under appropriate conditions (orifice diameters and spacing small compared to the mean free path, wall thickness small compared to the orifice diameters, etc.) the effusion can be described by the half-range Maxwellian

$$f_e^+ = \frac{n_e}{(2\pi RT_0)^{3/2}} \exp\left\{-\frac{\xi^2}{2RT_0}\right\} \quad , \qquad \xi_x > 0 \qquad (65)$$

with

$$n_e = qn_0 \qquad (66)$$

where q is the small, fractional porosity of the wall, and n_0 is the number density in the gas at stagnation conditions at the upstream side. In the limit of small porosity, capturing of impinging molecules can be neglected, and considering diffuse reflection, from the wall at temperature $T_w = T_0$, only we have

$$f_w^+ = \frac{n_w}{(2\pi RT_0)^{3/2}} \exp\left\{-\frac{\xi^2}{2RT_0}\right\} \quad , \qquad \xi_x > 0 \qquad (67)$$

i.e., the same half-range Maxwellian as above, except for the density.

The result of these two contributions is seen to be completely equivalent to the distribution function describing evaporation :

$$f_L^+ = \frac{n_L}{(2\pi RT_L)^{3/2}} \exp\{-\frac{\xi^2}{2RT_L}\} \quad , \qquad \xi_x > 0 \quad (3)$$

provided the temperature T_0 is taken to be T_L, and the sum of densities $n_e + n_w$ corresponds to n_L.

The conditions for the mass injection at the upstream boundary are thus the same in the two systems, and far downstream the state must approach a Maxwellian. The only lack of physical similarity between the two systems comes from the fact that molecules are reflected at the boundary in one case, and completely condensed into it in the other case. But this is merely a difference in physical processes taking place at the boundary itself and it does not affect the kinetics in the flow, as will be shown next.

7.2 Equivalent quantities. Transformation rules

The following considerations are general and are not limited by the approximate nature of the treatment of the evaporation problem in previous sections.

Assume that the one dimensional Boltzmann equation (4) can be solved for the half-space problem ($x > 0$) specified by

$$x = 0 : \quad f = f_\Omega^+ , \qquad \xi_x > 0 \qquad (68)$$

for given (pumping) conditions at macroscopic infinity. Then the solution may tend to a Maxwellian f_∞ (n_∞, u_∞, T_∞) far from the boundary.

The Maxwellian f_∞, describing the downstream equilibrium flow, will be the same in two physically different situations if the distribution function f_Ω^+ at the boundary is the same. The two flows will then be completely equivalent from the kinetic point of view.

For the two particular cases under consideration, the

condition for equivalence is given by Eqs. 65, 66 and 67 :

$$f_{\Omega}^{+} = f_{L}^{+} = f_{e}^{+} + f_{w}^{+} \tag{69}$$

which we rewrite as

$$f_{L}^{+} = (1+\alpha^{+})\, f_{e}^{+} \tag{70}$$

with α^{+} being defined as in previous treatments on effusive flow, i.e., as

$$\alpha^{+} = \frac{n_w}{n_e} \tag{71}$$

This gives the parameter relations

$$\begin{aligned} n_L &= (1+\alpha^{+})\, n_e \\ T_L &= T_0 \\ p_L &= (1+\alpha^{+})\, p_e \end{aligned} \tag{72}$$

Provided these relations are satisfied, the boundary conditions in the two problems are the same, and the flow field due to evaporation is completely equivalent to the corresponding effusive flow. In particular, the asymptotic downstream equilibrium state is the same in two cases.

This can be used to transform any result obtained in the effusive flow problem into an equivalent result for evaporation. We have, for instance, the relations

$$\frac{n_\infty}{n_L} = \frac{1}{1+\alpha^{+}} \frac{n_\infty}{n_e} \; ; \qquad \frac{T_\infty}{T_L} = \frac{T_\infty}{T_0} \; ;$$

$$\frac{p_\infty}{p_L} = \frac{1}{1+\alpha^{+}} \frac{p_\infty}{p_e} \; ; \qquad z_L = (1+\alpha^{+})\, z \tag{73}$$

that apply at constant u_∞, and therefore at constant S_∞.

The S_∞ versus z ($= qp_0/p_\infty$) relation in effusive flow is therefore transformed into the equivalent S_∞ versus z_L ($= p_L/p_\infty$) relation for evaporation by the simple change of driving parameter

$$z_L = (1+\alpha^+)z \qquad (74)$$

The transformation is practical in only one direction, namely from right to left, or from effusion to evaporation, because α^+ is an additional unknown that occurs in the effusion problem but not for evaporation provided the impinging molecules are all condensed at the interphase boundary.

For purpose of illustration, the solution corresponding to the approximating distribution function Eq. 6, ($\alpha^- = 0$, Ref. 30) for effusive flow has been included in Tables 3 and 4, so that it can be verified that the transformations above lead to the correct results.

7.3 Transformation of experimental results

The transformations from effusion to evaporation problems outlined above work equally well also for experimental quantities. This is of particular importance because many measurements are far more easily performed in the effusive flow than in the equivalent vapor flow problem.

We will now show that the transformation function α^+ in the expressions above can actually be obtained from simple flux measurements, so that the transformation of experimental results can be performed independent of any approximate theoretical treatments.

Consider the flux of molecules scattered back on the perforated wall in effusion

$$\int_{\xi_x<0} |\xi_x|\, f_w^-\, \underline{d\xi} \ .$$

In case of small wall porosity capturing of backscattered molecules by the wall orifices can be neglected, and we have the usual flux balance at a solid boundary:

$$\int_{\xi_x<0} |\xi_x|\, f_w^-\, \underline{d\xi} = \int_{\xi_x>0} \xi_x\, f_w^+\, \underline{d\xi} \qquad (75)$$

where $f_w^{\pm}$ is the distribution function for molecules that are brought in contact with the solid part of the wall.

According to the expression for f_w^+, Eq. 67, we have

$$\int_{\xi_x>0} \xi_x\, f_w^+\, \underline{d\xi} = \alpha^+\, n_e \sqrt{\frac{RT_0}{2\pi}} \equiv \alpha^+\, \dot{m}_e \qquad (76)$$

where the density n_w has been replaced by α^+ from the general definition, Eq. 71. But then Eq. 75 will give

$$\frac{\int_{\xi_x<0} |\xi_x|\, f_w^-\, \underline{d\xi}}{\dot{m}_e} = \alpha^+$$

and this is a quantity that was obtained experimentally in Ref. 30 at a variety of flow conditions, using a free molecular orifice probe mounted flush with the wall.

The transformation function α^+ is thus immediately available from already existing experimental data (Ref. 30), and transformation of experimental quantities can proceed in exactly the same way as for the theoretical results, i.e., by using the fundamental relations Eqs. 72, 73.

We now apply this result to obtain experimental information on two interesting quantities in evaporation:

backscattered flux at the interphase boundary $\dot{m}^-(0)$, and downstream speed ratio S_∞ as functions of the pressure ratio $z_L = \frac{p_L}{p_\infty}$.

For the flux we clearly have

$$\dot{m}^-(0) = \int_{\xi_x<0} |\xi_x| \, f_w^- \, d\underline{\xi} \qquad (78)$$

if the boundary conditions are equivalent, i.e., if

$$\dot{m}_L = \dot{m}_e \, (1+\alpha^+) \qquad (79)$$

Here the notation is such that

$$\dot{m}_L = n_L \sqrt{\frac{RT_L}{2\pi}} , \qquad \dot{m}_e = n_e \sqrt{\frac{RT_0}{2\pi}}$$

This gives for the backscattered flux in evaporation :

$$\frac{\dot{m}^-(0)}{\dot{m}_L} = \frac{1}{1+\alpha^+} \frac{\int_{\xi_x<0} |\xi_x| \, f_w^- \, d\underline{\xi}}{\dot{m}_e} = \frac{\alpha^+}{1+\alpha^+} \qquad (80)$$

in terms of the corresponding flux in effusion. The driving parameter is then transformed according to Eq. 74,

$$z_L = (1+\alpha^+) \, z \qquad (74)$$

where z is the pressure-porosity parameter in the perforated wall effusion.

All the information needed is therefore obtained from the experimental α^+ versus z-relation in Ref. 30 (Appendix 9, Test A-4), and the results are plotted in Fig. 15.

The theoretical results shown in the same figure are also transformed from Ref. 30 (although the case $\alpha^- = 0$ corres-

ponds to the present approximation, Eq. 6). The case $\alpha^- \neq 0$ corresponds to a more general expression for the distribution function;

$$f(x,\vec{\xi}) = a_1^+(x)f_L^+ + a_3^+(x)f_\infty^+ + a_3^-(x)f_\infty^- + a_4^-(x)f_*^- \qquad (81)$$

where the fourth mode f_*^- is the upstream tail of the Maxwellian that would result after BGK-first-collisions between evaporating (or effusing) molecules. The boundary value

$$a_4^-(0) = \alpha^-$$

is obtained from considerations of the probability for such collisions, and it may be shown (Ref. 30) that the expression

$$\alpha^- = \frac{n_e}{n_e+n_\infty}$$

represents an upper limit for this quantity in effusive flow. For evaporation this is equivalent to

$$\alpha^- = \frac{n_L}{n_L+n_\infty(1+\alpha^+)}$$

as indicated on the dash-dotted curve in Fig. 15.

The lower, dotted curve in the figure represents continuum theory and equilibrium results obtained by neglecting any non-equilibrium backscattering in the Knudsen layer ($\beta^- = 1$ in Eq. 21). These results are therefore completely equivalent to the Schrage formulation for the backscattered flux.

There is very good agreement between the kinetic theory results and the experiments throughout the whole range of flow conditions. The equilibrium theory underestimates in an important manner the backscattering that occurs, in particular at extreme conditions of strong evaporation. The experimental value at these conditions is

$$\frac{\dot{m}^{-}(0)}{\dot{m}_L} = 0.17 \pm 0.03 \qquad (S_\infty \simeq 0.9)$$

The resulting experimental band therefore covers the present theoretical results (0.180-0.185) the Monte-Carlo result of Ref. 18 (0.15), and the approximate non-linear result of Ref. 15 (0.189). The experimental value found by Gulubtsov seems to indicate a slightly lower value (0.13).

The experiments could possibly be repeated with better accuracy and at somewhat more clean conditions (less lateral expansion in the flow, higher Knudsen number for the effusion, etc.) to arrive at a more conclusive limiting value for the mass flux at strong evaporation.

Next the downstream speed ratio S_∞ is obtained as a function of z_L by simply using the transformation (74), again for the experimental data of Ref. 30 (Appendix 9, Test A-11). The results are shown on Fig. 16 in comparison with the same kind of theoretical predictions as discussed above. There is substantial agreement between kinetic theory results and experiments also for this quantity, and this proves in particular that z_L is the only relevant driving parameter in the problem.

The pressure-porosity parameter in the effusive flow $z = q \frac{p_0}{p_\infty}$ was defined experimentally by estimating the equilibrium pressure p_∞ from the ambient pressure p_t in the wind tunnel. Measurements of the static pressure locally in the equilibrium flow, assuming the temperature T_∞ to be correctly predicted by the theory, did indicate that this was a good approximation. In fact, the discrepancy between the static pressure thus found and the pressure measured outside the flow in the wind tunnel was always less than the most probable error in the experiments (Ref. 30).

Again the experimental accuracy can be considerably improved, so that even more conclusive results on the S_∞ versus z_L-relationship may be obtained.

8. CONCLUSIONS

A combined Mott-Smith, Liu-Lees method has been used to describe vapor motion at arbitrarily strong evaporation rates from a plane surface into a half-space.

Closed-form expressions have been obtained for the parameters of the downstream equilibrium flow, and for a non-equilibrium parameter describing backscattering into the phase boundary. There is one single driving parameter for the flow, most conveniently chosen as the pressure ratio $z_L = p_L/p_\infty$.

A simple improved version of the Hertz-Knudsen formula for the evaporated mass flux has been derived for use at weak, or moderately strong evaporation rates. The predicted mass flux is larger than the H-K value, by a factor close to 2.

At arbitrarily strong evaporation rates non-equilibrium effects are important, and Schrage's formula overestimates the mass flux. The present results give the relations between the downstream variables and the driving parameter that are missing in Schrage's formulation and account in addition for the non-equilibrium effects in a simple way. The limiting evaporation flux is $\dot{m}^+/\dot{m}_L = 0.82$ and is conditioned primarily by backscattering from non-equilibrium collisions.

The above conclusions are all independent of the physical properties of the vapor.

The x-dependence of the postulated trimodal distribution function in the Knudsen layer was obtained for a vapor consisting of Maxwell molecules. Spatial relaxation of the form $\exp(-\frac{x}{\ell})$ was found, where ℓ is a strongly increasing function of the downstream speed ratio, S_∞. At moderate flow conditions ℓ is of the same magnitude as λ_L, the mean free path for evaporating molecules, and the vapor expands at nearly constant temperature following a microscopic jump in temperature at the phase boundary. Extreme conditions occur at $S_\infty \simeq 0.91$, for which ℓ

goes to infinity and no equilibrium state is reached after a finite distance.

The present results are in good agreement with linearized kinetic theory predictions for weak evaporation, and with Monte Carlo and non-linear BGK results at arbitrarily large evaporation rates. This indicates that the present method yields an efficient description of the kinetics in vapor motion.

A simple analogy has been shown to exit between evaporation and the problem of effusion from a perforated boundary. It is demonstrated that experimental and theoretical information obtained in the latter problem can be directly transformed to the former, and the existing experimental data are in substantial agreement with the present theory.

It is suggested that more accurate measurements of backscattered flux at the wall in effusive flow are made at well defined conditions, so that more conclusive experimental information on evaporated mass flux can be obtained.

REFERENCES

1. HERTZ, H.: Ann. Physik, Vol. 17, 1882, p. 177.

2. KNUDSEN, M.: Ann. Physik, Vol. 47, 1915, p 697.

3. SCHRAGE, R.W.: A theoretical study of interphase mass transfer. Columbia U.Press, New York, 1953.

4. KUCHEROV, R.Ya.& RIEKENGLAS, L.E.: On hydrodynamic boundary conditions with evaporation of a solid absorbing radiant energy. Soviet Phys. JETP, Vol. 37, No 1, 1960, p. 10.

5. SHANKAR, P.N. & MARBLE, F.E.: Kinetic theory of transient condensation and evaporation at a plane surface. Phys.Fluids, Vol. 14, No 3, 1971, p 510.

6. LIU, C.H. & LEES, L.: Kinetic theory description of plane compressible Couette flow. in "Rarefied Gas Dynamics", L Talbot, ed., Academic Press, New York-London, 1961, p. 391.

7. PATTON, A.J. & SPRINGER, G.S.: A kinetic theory description of liquid vapor phase change. in "Rarefied Gas Dynamics", L. Trilling & H.Y. Wachman, eds., Academic Press, New York-London, 1969, p. 1497.

8. LOYALKA, S.K.: Approximate method in the kinetic theory. Phys. Fluids, Vol. 14, No 11, 1971, p. 2291.

9. CIPOLLA, J.W., LANG, H., LOYALKA, S.K.: Kinetic theory of evaporation and condensation. in "Rarefied Gas Dynamics", K. Karamcheti, ed., Academic Press, New York-London, 1972, p. 179.

10. PAO, Y.P.: Application of kinetic theory to the problem of evaporation and condensation. Phys. Fluids, Vol. 14, No 2, 1971, p. 306.

11. PAO, Y.P.: Temperature and density jumps in the kinetic theory of gases and vapors. Phys. Fluids, Vol. 14, No 7, 1971, p. 1340.

12. GAJEWSKI, P., KULICKI, A., WISNIEWSKI, A., ZGORZELSKI, M.: Kinetic theory approach to the vapor-phase phenomena in a non-equilibrium condensation process. Phys. Fluids, Vol. 17, No 2, 1974, p. 321.

13. ANISIMOV, S.I.: Vaporization of metal absorbing laser radiation. Soviet Phys. JETP, Vol. 27, No 1, 1958, p. 182.

14. LUIKOV, A.V., PERLEMAN, T.L., ANISIMOV, S.I.: Evaporation of a solid into vacuum. Int. J.Heat & Mass Transf., Vol. 14, No 2, 1971, p. 177.

15. EDWARDS, R.H. & COLLINS, R.L.: Evaporation from a spherical source into a vacuum.
in "Rarefied Gas Dynamics", L. Trilling & H.Y. Wachmann, eds, Academic Press, New York-London, 1969, p. 1489.

16. KOGAN, M.N. & MAKASHEV, N.K.: Fluid Dynamics, Vol. 6, No 6, 1974, p. 913.

17. MURAKAMI, M. & OSHIMA, K.: Kinetic approach to the transient evaporation and condensation problem.
in "Rarefied Gas Dynamics", M. Becker & M. Fiebig, eds., DFVLR Press, Porz-Wahn, 1974, Paper F.6.

18. MURAKAMI, M. & OSHIMA, K.: Kinetic approach to the evaporation and condensation problem.
ISAS, Tokyo, Report No 518, 1974, p. 261.

19. YEN, S.M.: Numerical solutions of non-linear kinetic equations for a one dimensional evaporation-condensation problem.
Computers & Fluids, Vol.1, No 4, 1973, p. 367.

20. YEN, S.M.: Solutions of kinetic equations for the non-equilibrium gas flow between emitting and absorbing surfaces.
in "Rarefied Gas Dynamics", M. Becker & M. Fiebig, eds., DFVLR Press, Porz-Wahn, 1974, Paper A.15.

21. MOTT-SMITH, H.M.: The solution of the Boltzmann equation for a shock wave.
Phys. Rev. Vol. 82, 1951, p. 885.

22. YTREHUS, T., SMOLDEREN, J.J., WENDT, J.F.: Mixing of thermal molecular jets produced from Knudsen effusion.
Entropie, No 42, 1971, p. 33.

23. YTREHUS, T.: A study of the large scale, rarefied flow fields that can be obtained through molecular effusion from a perforated boundary.
VKI TN 79, 1973.

24. YTREHUS, T.: One dimensional effusive flow by the method of moments.
in "Rarefied Gas Dynamics", M. Becker & M. Fiebig, eds., DFVLR Press, Porz-Wahn, 1974, Paper B.4.

25. VINCENTI, W.G. & KRUGER, C.H.: Introduction to physical gas dynamics.
J. Wiley, New York-London, 1965.

26. KOGAN, M.N.: Rarefied gas dynamics.
Plenum Press, New York, 1969.

27. CERCIGNANI, C.: Mathematical methods in kinetic theory.
Plenum Press, New York, 1969.

28. KOGAN, M.N.: Knudsen layer and its role in the gas and plasma flows.
(Review paper at Ninth Int. Symp. on RGD, Göttingen, 1974).
DFVLR Press, Porz-Wahn.

29. GOLUBTSOV, I.V.: Investigation of the evaporation of tantalum into vacua.
Heat Transfer-Soviet Res, Vol. 5, No 5, 1973, p. 18.

30. YTREHUS, T.: Theoretical and experimental study of a kinetic boundary layer produced by effusion from a perforated wall.
Doctoral Thesis, V.U.B., Brussels, 1975.

APPENDIX A

The conservation equations are obtained as moments of the Boltzmann equation with the collisional invariants as weight functions. We have from Eq. 9 :

$$\frac{\partial}{\partial x} \int \xi_x \, \psi_\mu \, f \, \underline{d\xi} = 0 \, , \qquad \mu = 1, 2, 3$$

so that

$$\int \xi_x \, \psi_\mu \, f \, \underline{d\xi} = C_\mu \qquad \text{(A-1)}$$

where the C_μ 's are the constant fluxes in the x-direction of mass, momentum and kinetic energy, respectively. Inserting the expression (6) for the distribution function, i.e.,

$$f = a_1^+ f_L^+ + a_3^+ f_\infty^+ + a_3^- f_\infty^- = \sum_{\nu=1}^{3} a_\nu(x) \, f_\nu \qquad \text{(A-2)}$$

we get the system of equations

$$\sum_{\nu=1}^{3} a_\nu(x) \, B\mu\nu = C_\mu \qquad \text{(A-3)}$$

with coefficients $B_{\mu\nu}$ defined as

$$B_{\mu\nu} = \int \xi_x \, \psi_\mu \, f_\nu \, \underline{d\xi} \, , \qquad \psi_\mu = 1, \, \xi_x, \, \frac{1}{2} \xi^2 \quad \text{for } \mu = 1,2,3 \qquad \text{(A-4)}$$

The f_ν 's are the half-range Maxwellians defined in Eqs. 3 and 5, i.e.

$$f_1 = f_L^+ = \frac{n_L}{(2\pi R T_L)^{3/2}} \exp\{-\frac{\xi^2}{2RT_L}\} \, , \quad \xi_x > 0$$

$$f_2 = f_\infty^+ = f_\infty, \; \xi_x > 0 \qquad \text{(A-4)}$$

$$f_3 = f_\infty^- = f_\infty, \; \xi_x < 0$$

with

$$f_\infty = \frac{n_\infty}{(2\pi RT_\infty)^{3/2}} \exp\left\{-\frac{(\xi_x - u_\infty)^2 + \xi_y^2 + \xi_z^2}{2RT_\infty}\right\}$$

Performing the integrations in velocity-space, in exactly the same manner as shown in great detail in Ref. 30, we have

$$B_{11} = n_L u_L, \qquad B_{12} = n_\infty \sqrt{\frac{RT_\infty}{2\pi}}\, \tilde{F}^+, \qquad B_{13} = -n_\infty \sqrt{\frac{RT_\infty}{2\pi}}\, \tilde{F}^-$$

$$B_{21} = \frac{1}{2} n_L RT_L, \qquad B_{22} = \frac{1}{2} n_\infty RT_\infty \tilde{G}^+, \qquad B_{23} = \frac{1}{2} n_\infty RT_\infty \tilde{G}^- \qquad \text{(A-6)}$$

$$B_{31} = 2n_L u_L RT_L, \qquad B_{32} = 2n_\infty \sqrt{\frac{RT_\infty}{2\pi}}\, RT_\infty \tilde{H}^+, \qquad B_{33} = -2n_\infty \sqrt{\frac{RT_\infty}{2\pi}}\, RT_\infty \tilde{H}^-$$

where $\tilde{F}^\pm$, $\tilde{G}^\pm$, and $\tilde{H}^\pm$ are dimensionless functions of the downstream speed ratio given in the following way [1]:

$$\tilde{F}^\pm = \sqrt{\pi}\, S_\infty (\pm 1 + \mathrm{erf} S_\infty) + e^{-S_\infty^2}$$

$$\tilde{G}^\pm = (2S_\infty^2 + 1)(1 \pm \mathrm{erf} S_\infty) \pm \frac{2}{\sqrt{\pi}} S_\infty e^{-S_\infty^2} \qquad \text{(A-7)}$$

$$\tilde{H}^\pm = \frac{\sqrt{\pi} S_\infty}{2} \left(S_\infty^2 + \frac{5}{2}\right)(\pm 1 + \mathrm{erf} S_\infty) + \frac{1}{2}(S_\infty^2 + 2)\, e^{-S_\infty^2}$$

The above definitions imply the relations

$$\tilde{F}^+ - \tilde{F}^- = 2\sqrt{\pi}\, S_\infty$$

$$\tilde{G}^+ + \tilde{G}^- = 4S_\infty^2 + 2 \qquad \text{(A-8)}$$

$$\tilde{H}^+ - \tilde{H}^- = \sqrt{\pi}\, S_\infty \left(S_\infty^2 + \frac{5}{2}\right)$$

---

[1] Note slightly different normalization compared to Refs. 23 and 30, e.g., $\tilde{F}^\pm = 2\sqrt{\pi}\, S_\infty \hat{F}^\pm$, $\tilde{G}^\pm = \hat{G}^\pm$, $\tilde{H}^\pm = \frac{\sqrt{\pi} S_\infty}{2} \hat{H}^\pm = \frac{1}{2\sqrt{\pi} S_\infty} H$.

By evaluating the constants C_μ at downstream equilibrium, we then can write the conservation equations in the following way :

$$n_L u_L \, a_1^+ \pm n_\infty \sqrt{\frac{RT_\infty}{RT_\infty}} \, \tilde{F}^\pm \, a_3^\pm = n_\infty u_\infty$$

$$\frac{1}{2} n_L RT_L \, a_1^+ + \frac{1}{2} n_\infty RT_\infty \, \tilde{G}^\pm \, a_3^\pm = n_\infty u_\infty^2 + n_\infty RT_\infty \qquad \text{(A-9)}$$

$$2n_L u_L RT_L \, a_1^+ \pm 2n_\infty \sqrt{\frac{RT_\infty}{2\pi}} \, RT_\infty \, \tilde{H}^\pm \, a_3^\pm = n_\infty u_\infty \left(\frac{1}{2} u_\infty^2 + \frac{5}{2} RT_\infty\right)$$

which in particular yield the Rankine-Hugoniot like equations (11) when the boundary conditions for the a_i 's at x = 0 are inserted.

The above conservation equations may also be considered as a system of three linear equations for the three amplitude functions a_1^+, a_3^+ and a_3^-. It is, however, clear that this system must not specify any non-trivial solution for the a_i 's, except at the boundaries, and thus we have the alternative condition

$$\text{Det} \quad || \, B_{\mu\nu} \, || = 0 \qquad \text{(A-10)}$$

which is completely equivalent to the Rankine-Hugoniot like relations between the boundary values.

Only two of the three conservation equations are therefore linearly independent in the present description of the flow, and the following relations between the amplitude functions are found to exist

$$a_3^+ = \frac{\beta^- - a_3^-}{\beta^- - 1} \quad , \qquad a_3^+ + a_1^+ = 1 \qquad \text{(A-11)}$$

where β^- is the value $a_3^-(0)$ at the phase boundary.

APPENDIX B - THE ξ_x^2-MOMENT EQUATION

We consider the transfer equation for ξ_x^2 in the case of Maxwell molecules and have (by Eq. 41)

$$\frac{\partial}{\partial x} \int \xi_x^3 f \, \underline{d\xi} = \frac{\pi}{\lambda_r m} \sqrt{\frac{RT_r}{2\pi}} \frac{n}{n_r} \tau'_{xx} \tag{B-1}$$

The equation must be expressed in terms of the amplitude functions and we first transform the collision term, working out the product $n\tau'_{xx}$. Let us write

$$\tau'_{xx} = \sum_{\nu=1}^{3} a_\nu (\tau'_{xx})_\nu \tag{B-2}$$

where the basic contributions are defined by

$$(\tau'_{xx})_\nu = -m\left[\int c_x c_x f_\nu \, \underline{dc} - \frac{1}{3} \int c^2 f_\nu \, \underline{dc}\right] \tag{B-3}$$

Making use of symmetry in velocity space, this can be written as

$$(\tau'_{xx})_\nu = -\frac{2}{3} m\left[\int c_x c_x f_\nu \, \underline{dc} - \int c_\perp^2 f \, \underline{dc}\right] \tag{B-4}$$

where c_x is the thermal velocity with respect to the local bulk velocity, i.e.

$$c_x \equiv \xi_x - u(x) \tag{B-5}$$

In complete analogy with the results of Refs. 23 and 27 we then get the separate contributions

$$(\tau'_{xx})_L = -\frac{2}{3} m \left[\frac{1}{2} n_L (-4uu_L + u^2)\right] \tag{B-6}$$

$$(\tau'_{xx})^{\pm}_{\infty} = -\frac{2}{3} m \left[\frac{1}{2} n_\infty RT_\infty \left(1 \pm \gamma\left(\frac{3}{2}, S_\infty^2\right)\right) \pm 2(u_\infty - u) n_\infty \sqrt{\frac{RT_\infty}{2\pi}}\, e^{-S_\infty^2} + (u_\infty - u)^2 \frac{1}{2} n_\infty (1 \pm \mathrm{erf} S_\infty) - \frac{1}{2} n_\infty RT_\infty (1 \pm \mathrm{erf} S_\infty)\right]$$

By collecting the terms containing u and u^2, respectively, in the resulting expression (B-2) and using the fact that the mass flux is constant throughout the flow field, i.e.,

$$nu = n_\infty u_\infty = \Sigma \tag{B-7}$$

we arrive at the result

$$\tau'_{xx} = -\frac{2}{3} m \left[-\frac{\Sigma^2}{n} + \frac{1}{2} n_\infty RT_\infty \{a_3^+ (\tilde{G}^+ - (1 + \mathrm{erf} S_\infty)) + a_3^- (\tilde{G}^- - (1 - \mathrm{erf} S_\infty))\}\right]$$

which we write as

$$n\tau'_{xx} = \frac{-\frac{2}{3} m\Sigma^2}{4S_\infty^2} \left[-4S_\infty^2 + \frac{n}{n_\infty} \{a_3^+ (\tilde{G}^+ - (1 + \mathrm{erf} S_\infty)) + a_3^- (\tilde{G}^- - (1 - \mathrm{erf} S_\infty))\}\right] \tag{B-8}$$

The density is given by

$$n = \int f \, \underline{d\xi} = \sum_{\nu=1}^{3} a_\nu \int f_\nu \, \underline{d\xi}$$

and may be expressed as

$$n = \frac{1}{2} n_L a_1^+ + \frac{1}{2} n_\infty (1 + \mathrm{erf} S_\infty) a_3^+ + \frac{1}{2} n_\infty (1 - \mathrm{erf} S_\infty) a_3^- \tag{B-9}$$

and the above expression for $n\tau'_{xx}$ is therefore a non-linear function in the a_i's that vanishes at downstream equilibrium.

By using the momentum conservation equation and the relation (A-11) between the amplitude functions, straightforward, but lengthy algebraic manipulations rendre the final expression

$$n\tau'_{xx} = \frac{\frac{2}{3} m\Sigma^2}{8S_\infty^2} \phi_1\phi_2(a_3^- - 1)(a_3^- - r) \qquad \text{(B-10)}$$

with ϕ_1, ϕ_2 and r being defined as

$$\phi_1 = \frac{1}{\beta^- - 1} \left[\frac{n_L}{n_\infty} - 2 + \beta^-(1-\text{erf}S_\infty)\right] \qquad \text{(B-11)}$$

$$\phi_2 = \frac{1}{\beta^- - 1} \left[z_L - 2 + \beta^-(1-\text{erf}S_\infty)\right]$$

$$r = 1 - \frac{2}{\phi_1} + \frac{4S_\infty^2}{\phi_2}$$

We next work out the convective term in the moment equation (B-1) which is

$$\frac{\partial}{\partial x} \int \xi_x^3 f \, \underline{d\xi} = \sum_{\nu=1}^{3} \frac{da_\nu}{dx} B_{4\nu} \qquad \text{(B-12)}$$

with the coefficients $B_{4\nu}$ being defined as

$$B_{4\nu} = \int \xi_x \psi_4 f_\nu \, \underline{d\xi} \qquad (\psi_4 = \xi_x^2) \qquad \text{(B-13)}$$

On performing the integrations in the velocity space, we have (again in complete analogy with Ref. 30)

$$B_{41} = 2n_L u_L RT_L \quad , \qquad B_{42} = 2n_\infty \sqrt{\frac{RT_\infty}{2\pi}} RT_\infty \tilde{K}^+ \qquad \text{(B-14)}$$

$$B_{43} = -2n_\infty \sqrt{\frac{RT_\infty}{2\pi}} RT_\infty \tilde{K}^-$$

where the functions $\tilde{K}^\pm$ are given by

$$\tilde{K}^\pm = (S_\infty^2 + \frac{3}{2})(\pm 1 + \text{erf}S_\infty) + (1+S_\infty^2) e^{-S_\infty^2} \qquad \text{(B-15)}$$

By using the simple relations (A-11) between the amplitude functions, the expression (B-12) can be written

$$\sum_{\nu=1}^{3} \frac{da_\nu}{dx} B_{4\nu} = \frac{1}{\bar{\beta}-1} \{2n_L u_L RT_L - 2n_\infty \sqrt{\frac{RT_\infty}{2\pi}}\, RT_\infty \left[\sqrt{\pi} S_\infty (2S_\infty^2+3) + \bar{\beta}\, \tilde{\bar{K}}\right]\} \frac{d\bar{a}_3}{dx} \qquad \text{(B-16)}$$

where the simple property

$$\tilde{K}^+ - \tilde{K}^- = \sqrt{\pi}\ S_\infty (2S_\infty^2+3) \qquad \text{(B-17)}$$

has also been applied.

It is possible (although not essential) to greatly simplify the above result by observing the additional relation

$$\tilde{K}^- = 2\tilde{H}^- - \tilde{F}^- \qquad \text{(B-18)}$$

and then using the Rankine-Hugoniot like equation (11) for mass and energy conservation to eliminate $\tilde{H}^-$ and $\tilde{F}^-$. Important cancelling then occurs among the terms, and the final result for the convective term is

$$\sum_{\nu=1}^{3} \frac{da_\nu}{dx} B_{4\nu} = -\frac{2n_L u_L RT_L}{\bar{\beta}-1} \left(1 - \frac{T_\infty}{T_L}\right) \frac{d\bar{a}_3}{dx} \qquad \text{(B-19)}$$

APPENDIX C - USEFUL INTEGRALS

In performing the integrations of the various half-range Gaussian distribution functions in previous appendices, frequent use was made of the following properties of gamma functions.

Complete gamma functions $\Gamma(z)$:

$$\Gamma(z) = \int_0^\infty e^{-t}\, t^{z-1}\, dt$$

$$\Gamma(z) = (z-1)! \qquad \text{(C-1)}$$

$$\Gamma(z+1) = z\Gamma(z) \quad , \quad \Gamma(\tfrac{1}{2}) = \sqrt{\pi}$$

Particular integral

$$\int_{-\infty}^{+\infty} t^n\, e^{-\beta t^2}\, dt = \begin{cases} 0 & n \text{ odd} \\ \beta^{-\frac{n+1}{2}}\, \Gamma(\frac{1}{2}) & n \text{ even} \end{cases} \qquad \text{(C-2)}$$

Incomplete gamma functions $\Gamma(z,x)$, $\gamma(z,x)$:

$$\Gamma(z,x) = \int_0^x e^{-t}\, z^{t-1}\, dt$$

$$\gamma(z,x) = \frac{1}{\Gamma(z)}\, \Gamma(z,x) \qquad \text{(C-3)}$$

Recursion formula

$$\gamma(z+1,x) = \gamma(z,x) - \frac{x^z\, e^{-x}}{\Gamma(z+1)} \qquad \text{(C-4)}$$

Particular case : $z = \frac{1}{2}$, $x = S_\infty^2$

$$\gamma\left(\frac{3}{2} , S_\infty^2\right) = \gamma\left(\frac{1}{2} , S_\infty^2\right) - \frac{1}{\Gamma\left(\frac{3}{2}\right)} \; S_\infty \; e^{-S_\infty^2} \qquad \text{(C-5)}$$

with

$$\gamma\left(\frac{1}{2} , S_\infty^2\right) = \frac{2}{\sqrt{\pi}} \int_0^{S_\infty} e^{-u^2} du \equiv \text{erf } S_\infty \qquad \text{(C-6)}$$

TABLE 1 - GAS DYNAMIC PARAMETERS FOR EVAPORATION

***** E V A P O R A T I O N C O N D E N S A T I O N *****

(GAS DYNAMIC PARAMETERS)

ROOT NO.2

S	z_L	n_∞/n_L	T_∞/T_L	$\dot{m}^+_{(o)}/\dot{m}_L$	$\frac{\dot{q}_w}{2n_L u_L R T_L}$	$\dot{m}^+_{(o)}/\dot{m}^-_{(o)}$	BF
.00	1.00000+00	0.00000	1.00000+00	0.00000	0.00000	1.00000+00	0.00000
.05	1.11073+00	9.20476-01	9.78088-01	1.61353-01	1.97469-01	1.19240+00	5.86361-04
.10	1.23070+00	8.49358-01	9.56660-01	2.94493-01	3.53570-01	1.41742+00	2.35823-03
.15	1.36035+00	7.85613-01	9.35705-01	4.04087-01	4.76886-01	1.67810+00	5.32126-03
.20	1.50016+00	7.28349-01	9.15217-01	4.94011-01	5.74201-01	1.97633+00	9.45818-03
.25	1.65056+00	6.76792-01	8.95188-01	5.67489-01	6.50887-01	2.31208+00	1.47223-02
.30	1.81200+00	6.30277-01	8.75608-01	6.27209-01	7.11200-01	2.68247+00	2.10282-02
.35	1.98494+00	5.88220-01	8.56471-01	6.75413-01	7.58521-01	3.08084+00	2.82444-02
.40	2.16980+00	5.50118-01	8.37768-01	7.13975-01	7.95533-01	3.49620+00	3.61847-02
.45	2.36702+00	5.15531-01	8.19491-01	7.44465-01	8.24373-01	3.91335+00	4.46042-02
.50	2.57700+00	4.84072-01	8.01632-01	7.68197-01	8.46740-01	4.31400+00	5.31982-02
.55	2.80017+00	4.55405-01	7.84183-01	7.86274-01	8.63986-01	4.67889+00	6.16082-02
.60	3.03692+00	4.29234-01	7.67136-01	7.99624-01	8.77191-01	4.99063+00	6.94335-02
.65	3.28764+00	4.05297-01	7.50484-01	8.09027-01	8.87214-01	5.23633+00	7.62501-02
.70	3.55271+00	3.83367-01	7.34218-01	8.15137-01	8.94740-01	5.40942+00	8.16321-02
.75	3.83249+00	3.63241-01	7.18331-01	8.18509-01	9.00314-01	5.50990+00	8.51751-02
.80	4.12732+00	3.44739-01	7.02816-01	8.19607-01	9.04372-01	5.54346+00	8.65164-02
.85	4.43756+00	3.27702-01	6.87664-01	8.18826-01	9.07258-01	5.51955+00	8.53497-02
.90	4.76352+00	3.11991-01	6.72868-01	8.16496-01	9.09247-01	5.44947+00	8.14341-02
.95	5.10553+00	2.97478-01	6.58422-01	8.12898-01	9.10559-01	5.34467+00	7.45976-02
1.00	5.46387+00	2.84054-01	6.44316-01	8.08267-01	9.11364-01	5.21559+00	6.47332-02
1.05	5.83884+00	2.71617-01	6.30545-01	8.02804-01	9.11800-01	5.07111+00	5.17950-02
1.10	6.23071+00	2.60080-01	6.17100-01	7.96677-01	9.11973-01	4.91828+00	3.57891-02
1.15	6.63974+00	2.49362-01	6.03975-01	7.90027-01	9.11966-01	4.76253+00	1.67651-02
1.20	7.06618+00	2.39391-01	5.91163-01	7.82975-01	9.11846-01	4.60777+00	-5.19294-03

∇FIN

TABLE 2 - KINETIC PARAMETERS FOR EVAPORATION

***** E V A P O R A T I O N C O N D E N S A T I O N *****

(KINETIC PARAMETERS)

ROOT NO.2

S	β^-	r	C/B	λ_L/ℓ	λ_L/ℓ_n	ϕ_1	ϕ_2
.05	1.00807+00	5.72483-01	2.86204+00	1.22357+00	1.24667+00	4.66397+00	7.67984+00
.10	1.01982+00	5.25278-01	2.35656+00	1.11872+00	1.16543+00	4.16182+00	6.85298+00
.15	1.03650+00	4.75089-01	1.94101+00	1.01886+00	1.08970+00	3.70605+00	6.10248+00
.20	1.05973+00	4.22186-01	1.59905+00	9.23950-01	1.01946+00	3.29316+00	5.42261+00
.25	1.09163+00	3.67043-01	1.31745+00	8.33887-01	9.54599-01	2.91991+00	4.80801+00
.30	1.13494+00	3.10395-01	1.08541+00	7.48504-01	8.94969-01	2.58318+00	4.25354+00
.35	1.19323+00	2.53344-01	8.94120-01	6.67600-01	8.40374-01	2.28006+00	3.75442+00
.40	1.27113+00	1.97468-01	7.36354-01	5.90947-01	7.90596-01	2.00780+00	3.30611+00
.45	1.37462+00	1.44987-01	6.06201-01	5.18310-01	7.45405-01	1.76382+00	2.90435+00
.50	1.51146+00	9.89712-02	4.98815-01	4.49444-01	7.04568-01	1.54568+00	2.54516+00
.55	1.69171+00	6.36128-02	4.10205-01	3.84109-01	6.67849-01	1.35111+00	2.22479+00
.60	1.92839+00	4.45857-02	3.37094-01	3.22064-01	6.35020-01	1.17801+00	1.93975+00
.65	2.23841+00	4.95162-02	2.76787-01	2.63082-01	6.05858-01	1.02438+00	1.68678+00
.70	2.64369+00	8.86002-02	2.27056-01	2.06939-01	5.80149-01	8.88403-01	1.46287+00
.75	3.17270+00	1.75419-01	1.86066-01	1.53426-01	5.57692-01	7.68358-01	1.26520+00
.80	3.86246+00	3.28009-01	1.52299-01	1.02344-01	5.38294-01	6.62672-01	1.09118+00
.85	4.76115+00	5.70266-01	1.24502-01	5.35029-02	5.21775-01	5.69888-01	9.38394-01
.90	5.93157+00	9.33809-01	1.01639-01	6.72757-03	5.07967-01	4.88664-01	8.04648-01
.95	7.45565+00	1.46044+00	8.28513-02	-3.81479-02	4.96711-01	4.17768-01	6.87910-01
1.00	9.44052+00	2.20538+00	6.74294-02	-8.12779-02	4.87861-01	3.56074-01	5.86321-01
1.05	1.20264+01	3.24160+00	5.47853-02	-1.22807-01	4.81280-01	3.02550-01	4.98189-01
1.10	1.53973+01	4.66553+00	4.44324-02	-1.62868-01	4.76841-01	2.56262-01	4.21969-01
1.15	1.97950+01	6.60468+00	3.59678-02	-2.01588-01	4.74427-01	2.16359-01	3.56263-01
1.20	2.55377+01	9.22779+00	2.90577-02	-2.39080-01	4.73929-01	1.82072-01	2.99806-01

VFIN

TABLE 3 - GAS DYNAMIC PARAMETERS FOR EFFUSION ($\alpha^- = 0$)

VXQT A

***** S I M P L E C A S E *****

POSITIVE ROOT

S	Z	T3/T0	N3/N1	SIGM/2	EPS/2	BF
.10	3.62432-01	9.56660-01	2.88414+00	2.31432+00	1.00304-01	3.12984-02
.20	7.41093-01	9.15217-01	1.47436+00	9.57307-01	8.11630-02	5.71911-02
.30	1.13650+00	8.75608-01	1.00489+00	5.38271-01	6.69564-02	8.09985-02
.40	1.54918+00	8.37768-01	7.70501-01	3.52061-01	5.71157-02	1.05070-01
.50	1.97965+00	8.01632-01	6.30141-01	2.57711-01	5.11218-02	1.30493-01
.60	2.42840+00	7.67136-01	5.36794-01	2.08286-01	4.85022-02	1.56943-01
.70	2.89595+00	7.34218-01	4.70310-01	1.83714-01	4.88280-02	1.82875-01
.80	3.38278+00	7.02816-01	4.20615-01	1.74001-01	5.17104-02	2.06078-01
.90	3.88940+00	6.72868-01	3.82109-01	1.73626-01	5.67986-02	2.24341-01
1.00	4.41627+00	6.44316-01	3.51436-01	1.79306-01	6.37765-02	2.35933-01
1.10	4.96386+00	6.17100-01	3.26456-01	1.88979-01	7.23602-02	2.39784-01
1.20	5.53264+00	5.91163-01	3.05746-01	2.01293-01	8.22958-02	2.35438-01
1.30	6.12305+00	5.66450-01	2.88317-01	2.15330-01	9.33565-02	2.22911-01
1.40	6.73551+00	5.42906-01	2.73467-01	2.30457-01	1.05340-01	2.02538-01
1.50	7.37046+00	5.20479-01	2.60677-01	2.46222-01	1.18069-01	1.74850-01
1.60	8.02830+00	4.99117-01	2.49559-01	2.62303-01	1.31383-01	1.40478-01
1.70	8.70943+00	4.78772-01	2.39818-01	2.78467-01	1.45145-01	1.00098-01
1.80	9.41422+00	4.59395-01	2.31222-01	2.94542-01	1.59231-01	5.43856-02
1.90	1.01431+01	4.40940-01	2.23590-01	3.10407-01	1.73536-01	3.99171-03
2.00	1.08963+01	4.23364-01	2.16774-01	3.25970-01	1.87966-01	-5.04683-02
2.10	1.16742+01	4.06623-01	2.10659-01	3.41169-01	2.02442-01	-1.08424-01
2.20	1.24772+01	3.90678-01	2.05146-01	3.55959-01	2.16894-01	-1.69355-01
2.30	1.33056+01	3.75488-01	2.00156-01	3.70310-01	2.31263-01	-2.32785-01
2.40	1.41597+01	3.61016-01	1.95623-01	3.84202-01	2.45499-01	-2.98289-01
2.50	1.50397+01	3.47227-01	1.91491-01	3.97627-01	2.59560-01	-3.65481-01
2.60	1.59459+01	3.34087-01	1.87712-01	4.10579-01	2.73410-01	-4.34022-01
2.70	1.68786+01	3.21561-01	1.84247-01	4.23062-01	2.87021-01	-5.03607-01
2.80	1.78381+01	3.09621-01	1.81060-01	4.35078-01	3.00369-01	-5.73967-01
2.90	1.88245+01	2.98235-01	1.78122-01	4.46638-01	3.13435-01	-6.44865-01
3.00	1.98382+01	2.87375-01	1.75408-01	4.57750-01	3.26204-01	-7.16092-01

VFIN

TABLE 4 - KINETIC PARAMETERS FOR EFFUSION ($\alpha^- = 0$)

VXGT A

***** S I M P L E C A S E *****

POSITIVE ROOT,TAB.2

S	BETA-	ALFA+	R	B	OMEGA1	LAM1/LG
.05	1.00807+00	5.19760+00	5.72480-01	1.68278+01	7.58318+00	7.72632+00
.10	1.01982+00	2.39567+00	5.25277-01	7.42528+00	3.79881+00	3.95741+00
.15	1.03650+00	1.47472+00	4.75088-01	4.35953+00	2.52138+00	2.69670+00
.20	1.05973+00	1.02425+00	4.22186-01	2.87340+00	1.87030+00	2.06363+00
.25	1.09163+00	7.62148-01	3.67043-01	2.01575+00	1.46943+00	1.68215+00
.30	1.13494+00	5.94365-01	3.10396-01	1.46974+00	1.19339+00	1.42691+00
.35	1.19323+00	4.80576-01	2.53344-01	1.09973+00	9.88432-01	1.24424+00
.40	1.27113+00	4.00609-01	1.97468-01	8.38058-01	8.27686-01	1.10732+00
.45	1.37462+00	3.43247-01	1.44987-01	6.47238-01	6.96218-01	1.00126+00
.50	1.51146+00	3.01750-01	9.89711-02	5.04879-01	5.85064-01	9.17171-01
.55	1.69171+00	2.71821-01	6.36127-02	3.96816-01	4.88517-01	8.49385-01
.60	1.92839+00	2.50587-01	4.45855-02	3.13678-01	4.02770-01	7.94148-01
.65	2.23841+00	2.36053-01	4.95155-02	2.49041-01	3.25183-01	7.48872-01
.70	2.64369+00	2.26787-01	8.85997-02	1.98370-01	2.53870-01	7.11720-01
.75	3.17270+00	2.21734-01	1.75419-01	1.58386-01	1.87446-01	6.81351-01
.80	3.86246+00	2.20097-01	3.28009-01	1.26672-01	1.24869-01	6.56771-01
.85	4.76115+00	2.21261-01	5.70265-01	1.01417-01	6.53411-02	6.37224-01
.90	5.93157+00	2.24746-01	9.33809-01	8.12426-02	8.23956-03	6.22130-01
.95	7.45565+00	2.30167-01	1.46044+00	6.50901-02	-4.69283-02	6.11038-01
1.00	9.44052+00	2.37215-01	2.20538+00	5.21363-02	-1.00558-01	6.03589-01
1.05	1.20264+01	2.45634-01	3.24160+00	4.17366-02	-1.52972-01	5.99498-01
1.10	1.53974+01	2.55214-01	4.66553+00	3.33826-02	-2.04435-01	5.98537-01
1.15	1.97950+01	2.65779-01	6.60468+00	2.66709-02	-2.55165-01	6.00519-01
1.20	2.55377+01	2.77180-01	9.22780+00	2.12798-02	-3.05349-01	6.05292-01
1.25	3.30455+01	2.89290-01	1.27584+01	1.69519-02	-3.55140-01	6.12731-01
1.30	4.28736+01	3.02000-01	1.74931+01	1.34806-02	-4.04674-01	6.22731-01
1.35	5.57578+01	3.15217-01	2.38259+01	1.06995-02	-4.54062-01	6.35205-01
1.40	7.26756+01	3.28858-01	3.22807+01	8.47447-03	-5.03405-01	6.50080-01

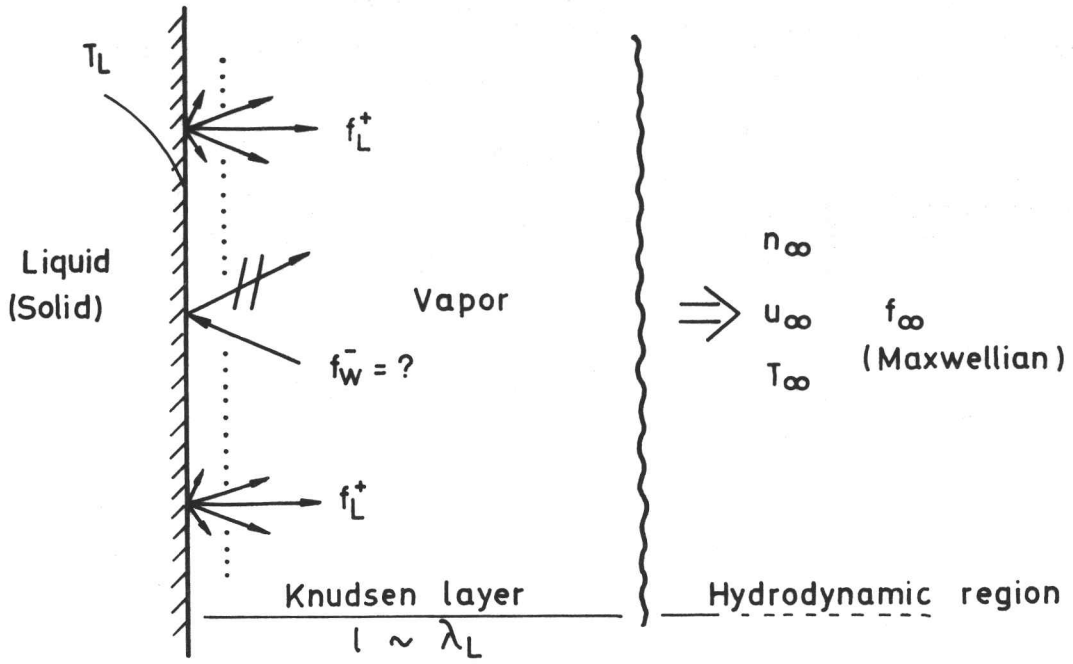

FIG. 1 DEFINITION OF HALF-SPACE EVAPORATION CONDENSATION PROBLEM

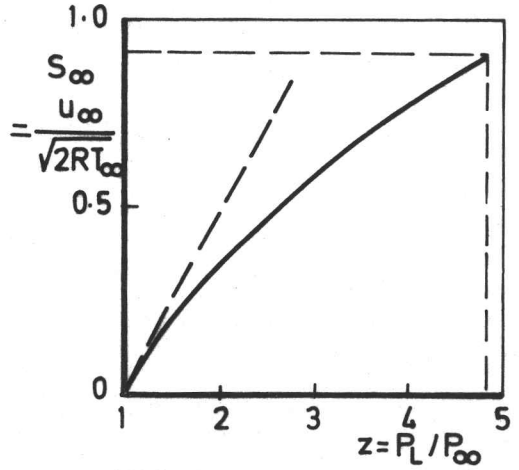

FIG. 2 a)

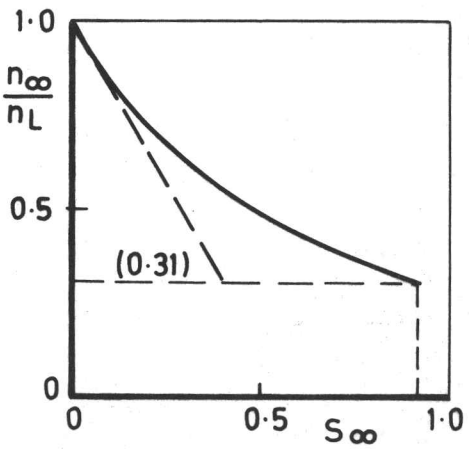

FIG. 2 b)

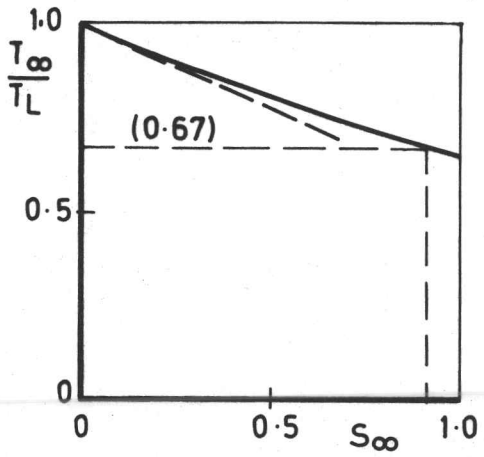

FIG. 2 c)

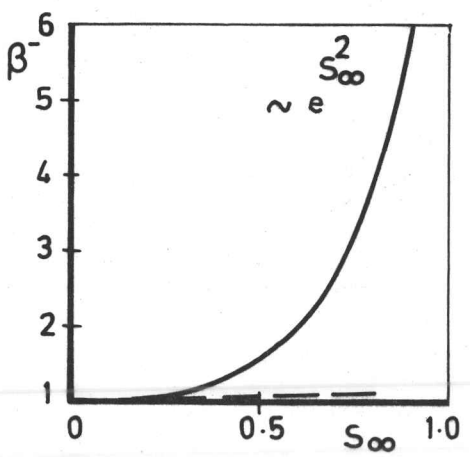

FIG. 2 d)

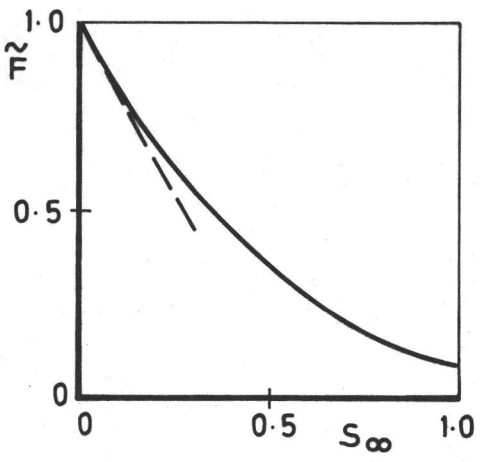

FIG. 2 e)

FIG. 2 RESULTS FROM GAS DYNAMIC CALCULATIONS

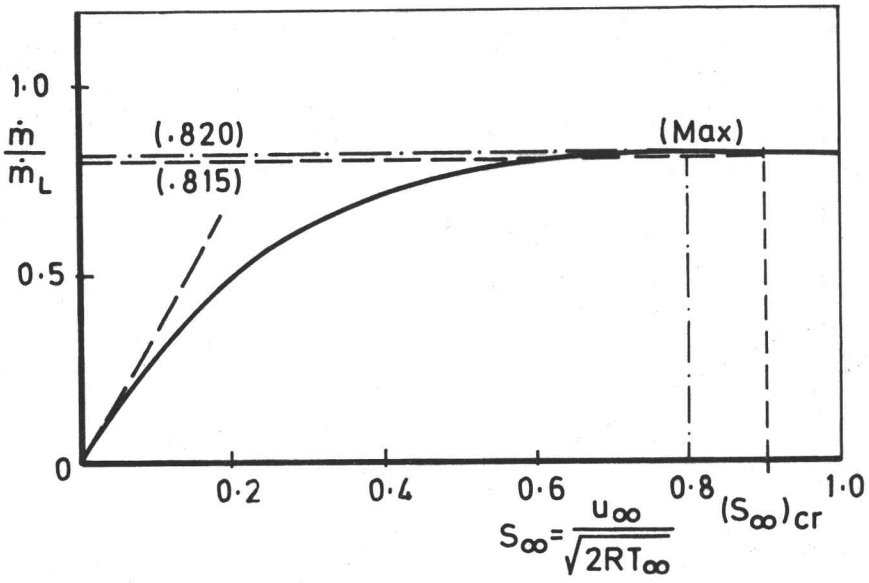

FIG. 3 NORMALIZED MASS FLUX VERSUS DOWNSTREAM SPEED RATIO

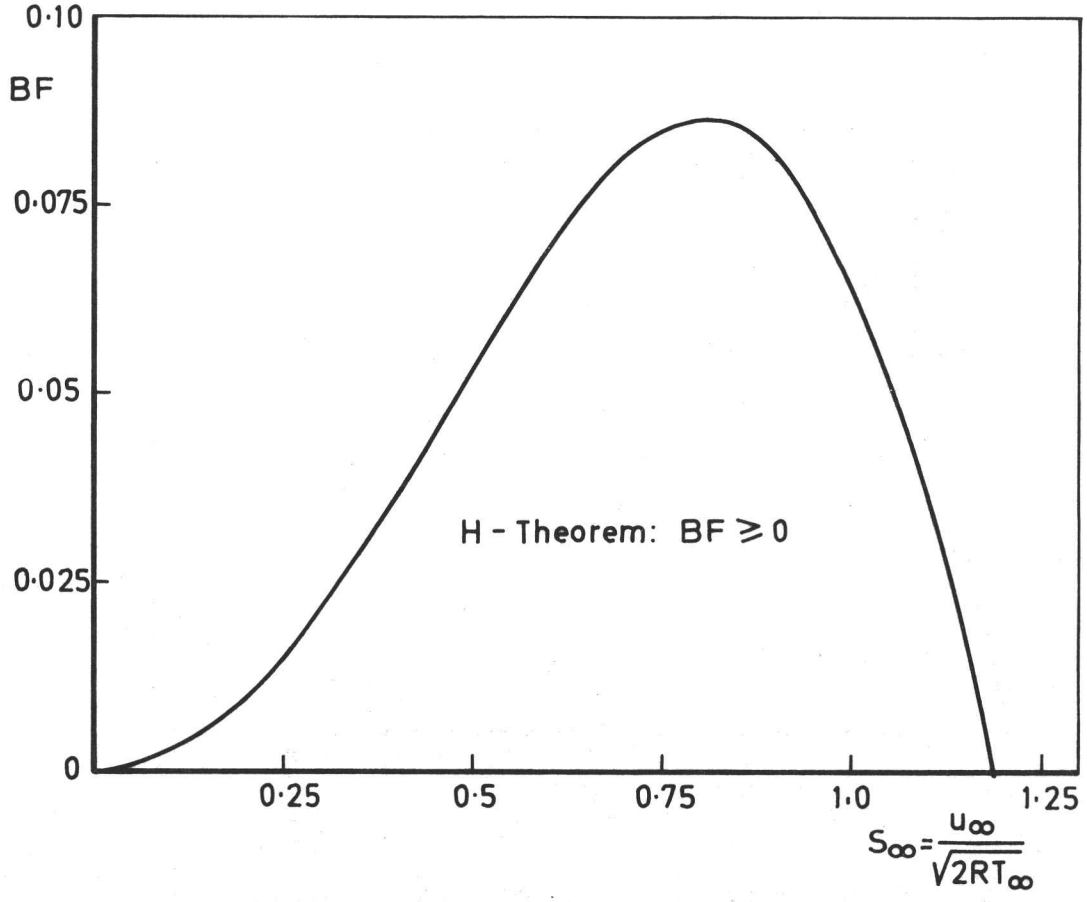

FIG. 4 RESULTS FROM THE BOLTZMANN H-THEOREM

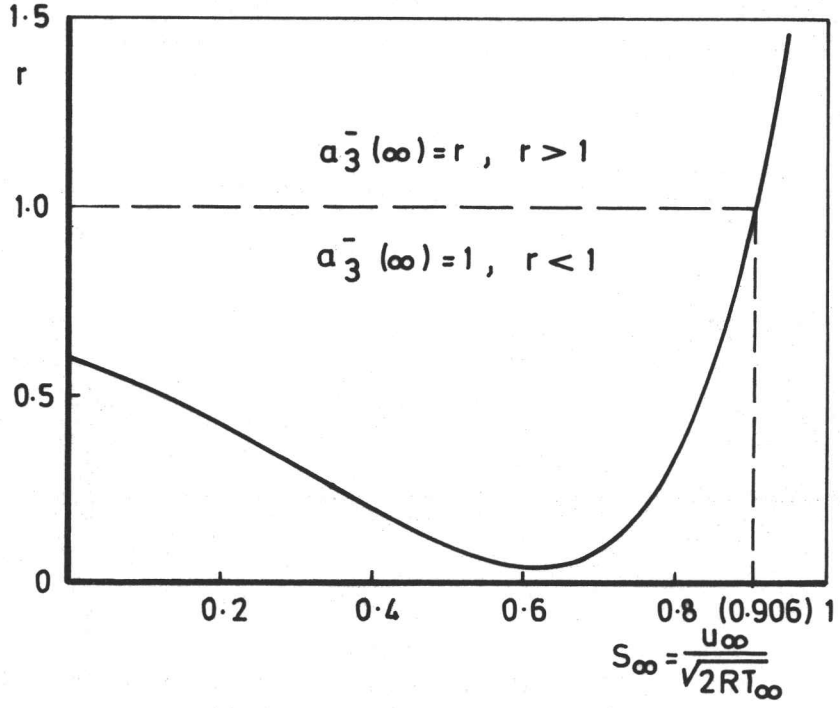

FIG. 5 SPURIOUS EQUILIBRIUM PARAMETER IN ξ_x^2 - MOMENT EQUATION

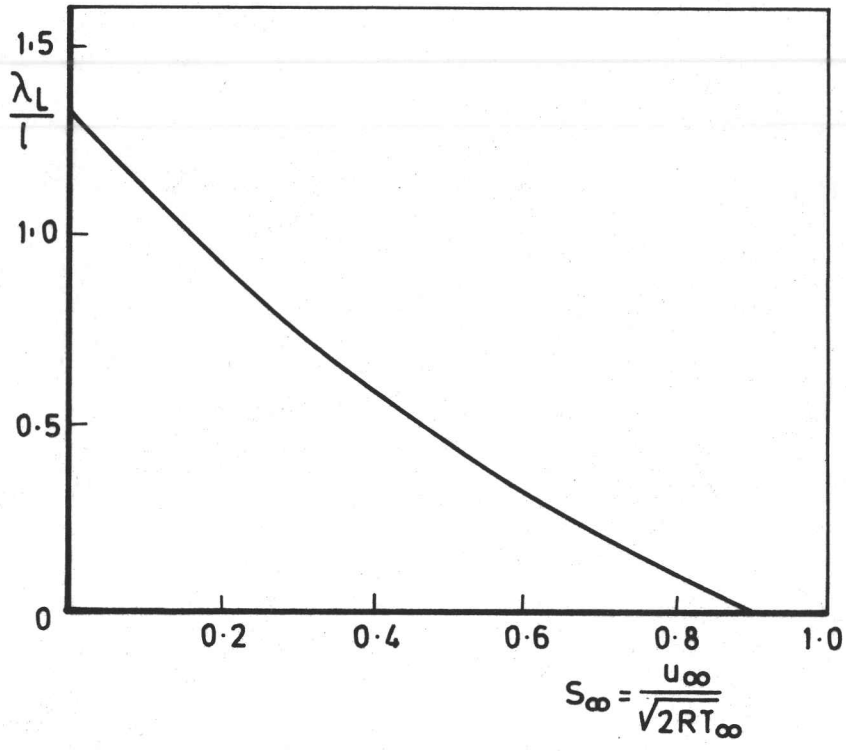

FIG. 6 RECIPROCAL THICKNESS SCALE FOR THE VAPOR KNUDSEN LAYER

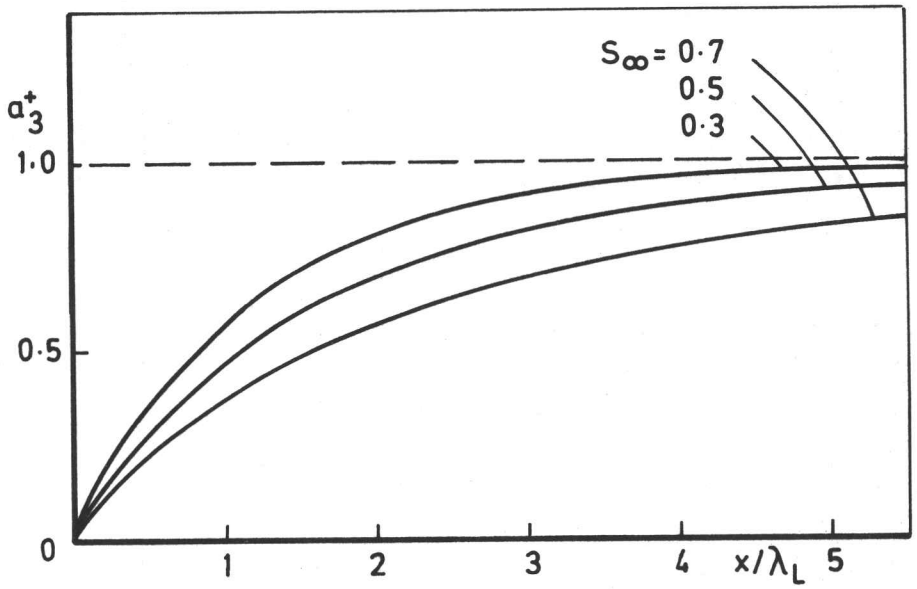

FIG. 7 RELAXATION OF THE MODE a_3^+ AT VARIOUS FLOW CONDITIONS

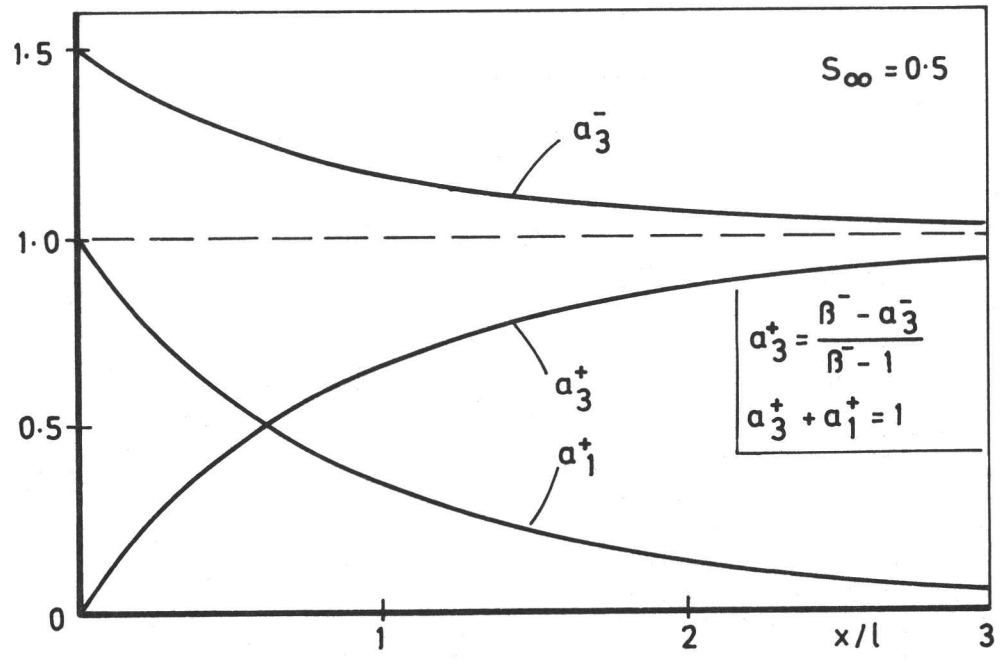

FIG. 8 RELAXATION OF BASIC MODES AT S_∞ = 0·5

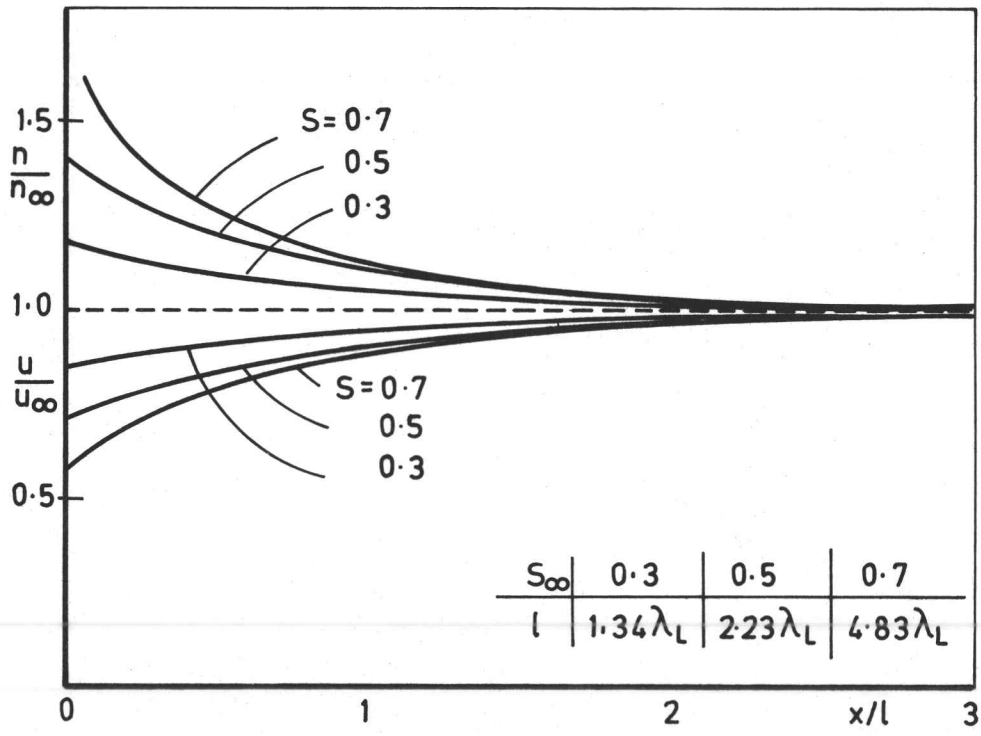

FIG. 9 DENSITY AND VELOCITY PROFILES IN THE VAPOR KNUDSEN LAYER

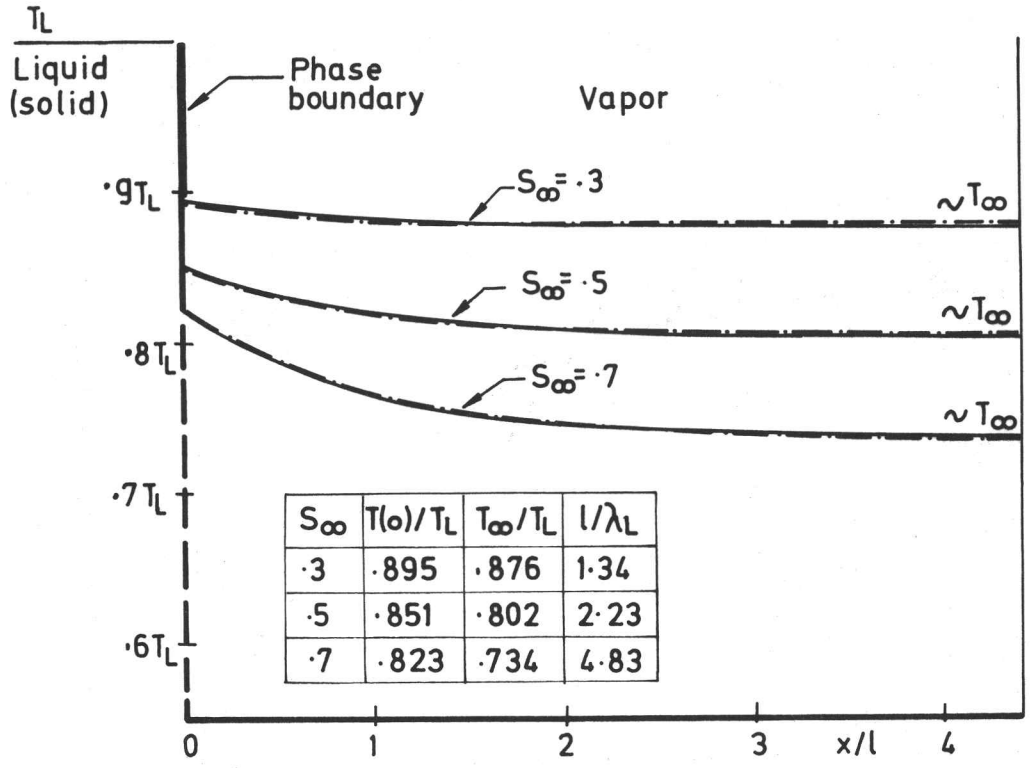

S_∞	$T(o)/T_L$	T_∞/T_L	l/λ_L
·3	·895	·876	1·34
·5	·851	·802	2·23
·7	·823	·734	4·83

FIG. 10 TEMPERATURE PROFILES IN VAPOR KNUDSEN LAYER EXHIBITING MICROSCOPIC JUMP AT THE PHASE BOUNDARY

$\alpha^- = 0$

S	$T(o)/T_o$	T_M/T_o	l/λ_1
·3	·8949	·8756	·8379
·5	·8509	·8016	1·7092
·7	·8229	·7342	3·9390

$\alpha^- = \frac{n_e}{n_e + n_M}$

S	$T(o)/T_o$	T_M/T_o	l/λ_1
·3	·8910	·8814	1·9611
·5	·8490	·8040	3·9737
·7	·8273	·7307	8·3019

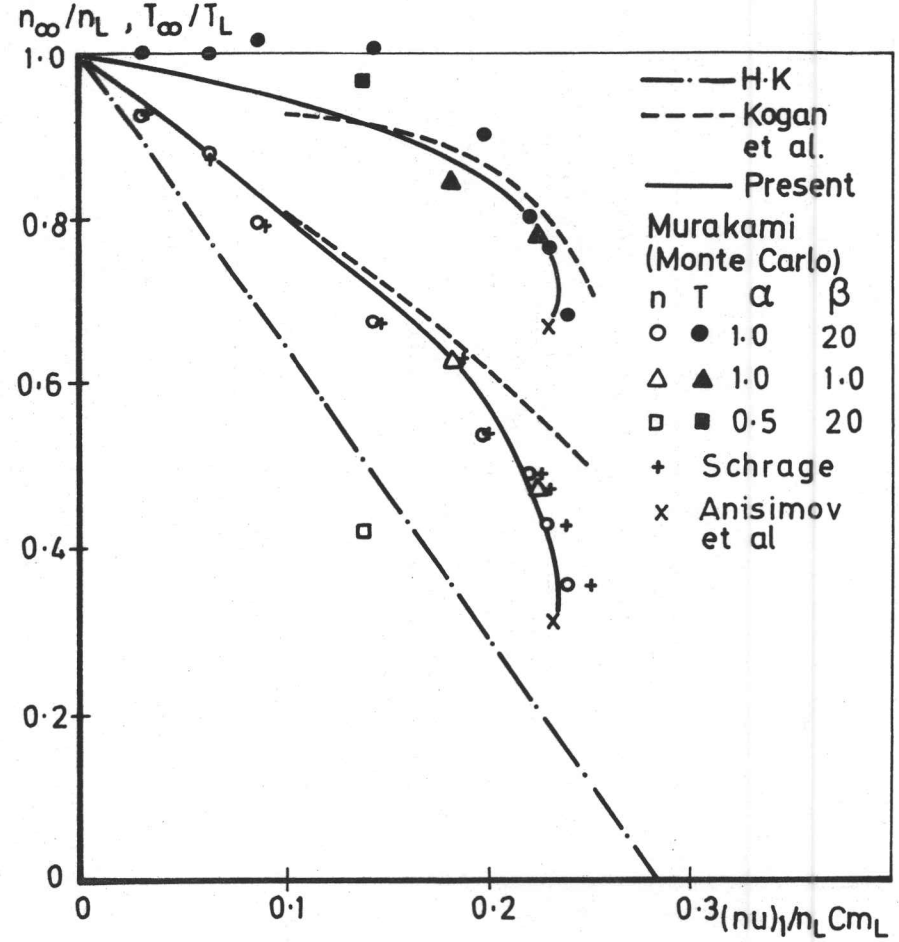

FIG. 11 DOWNSTREAM NUMBER DENSITY AND TEMPERATURE VERSUS NUMBER FLUX RATE. COMPARISON WITH NUMERICAL RESULTS

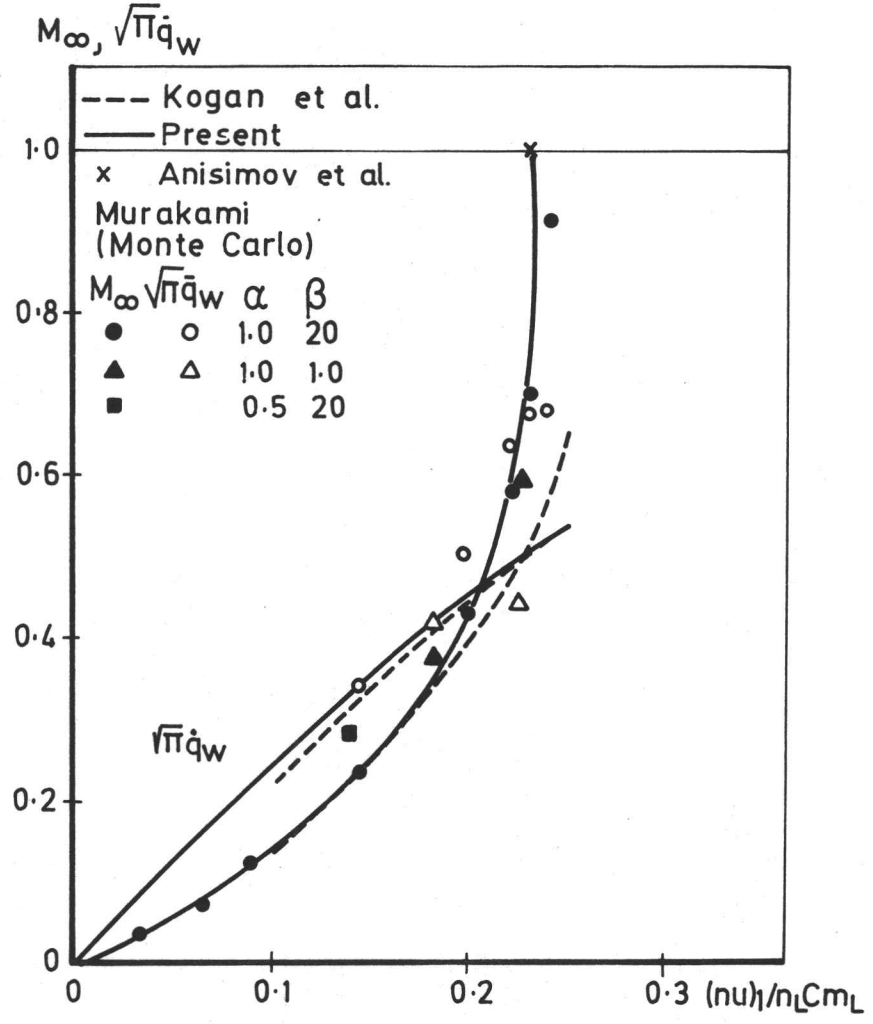

FIG.12 DOWNSTREAM MACH NUMBER AND HEAT FLUX FROM PHASE BOUNDARY VERSUS NUMBER FLUX RATE. COMPARISON WITH NUMERICAL RESULTS

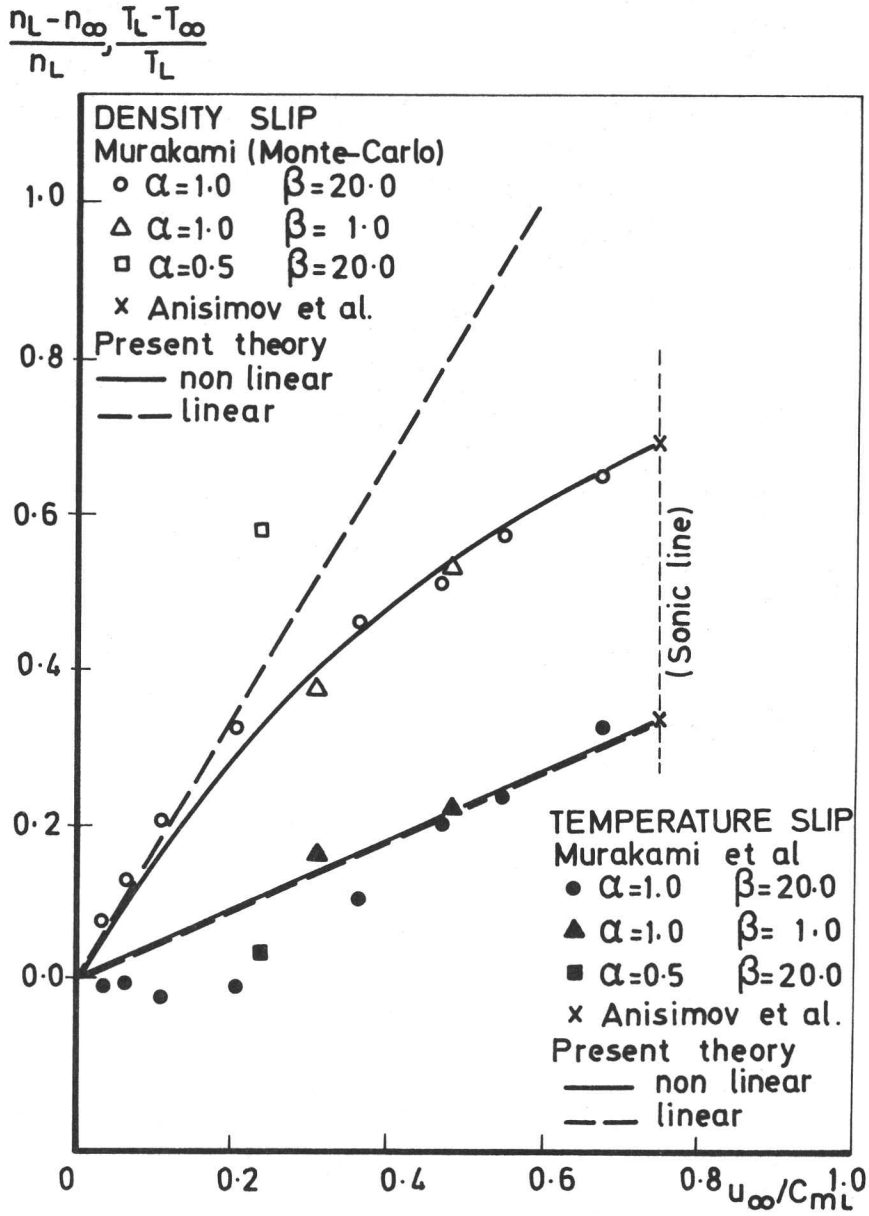

FIG. 13 MACROSCOPIC JUMPS IN NUMBER DENSITY AND TEMPERATURE THROUGH VAPOR KNUDSEN LAYER

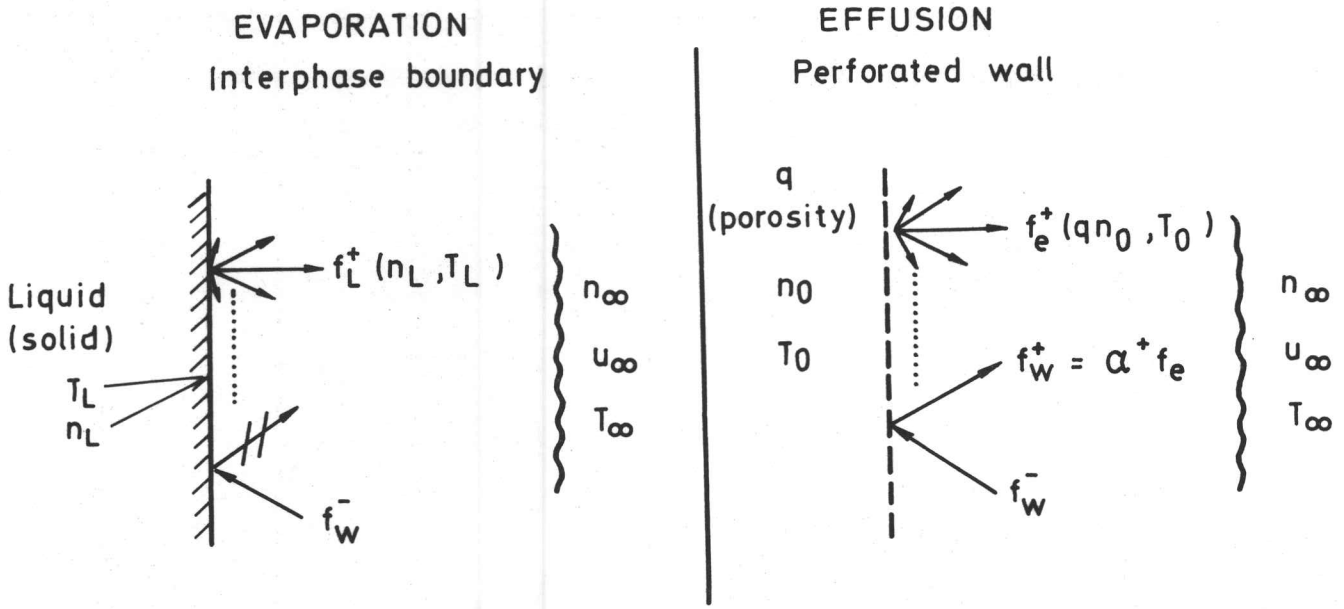

FIG. 14 PHYSICAL MODELS FOR EVAPORATION AND EFFUSION

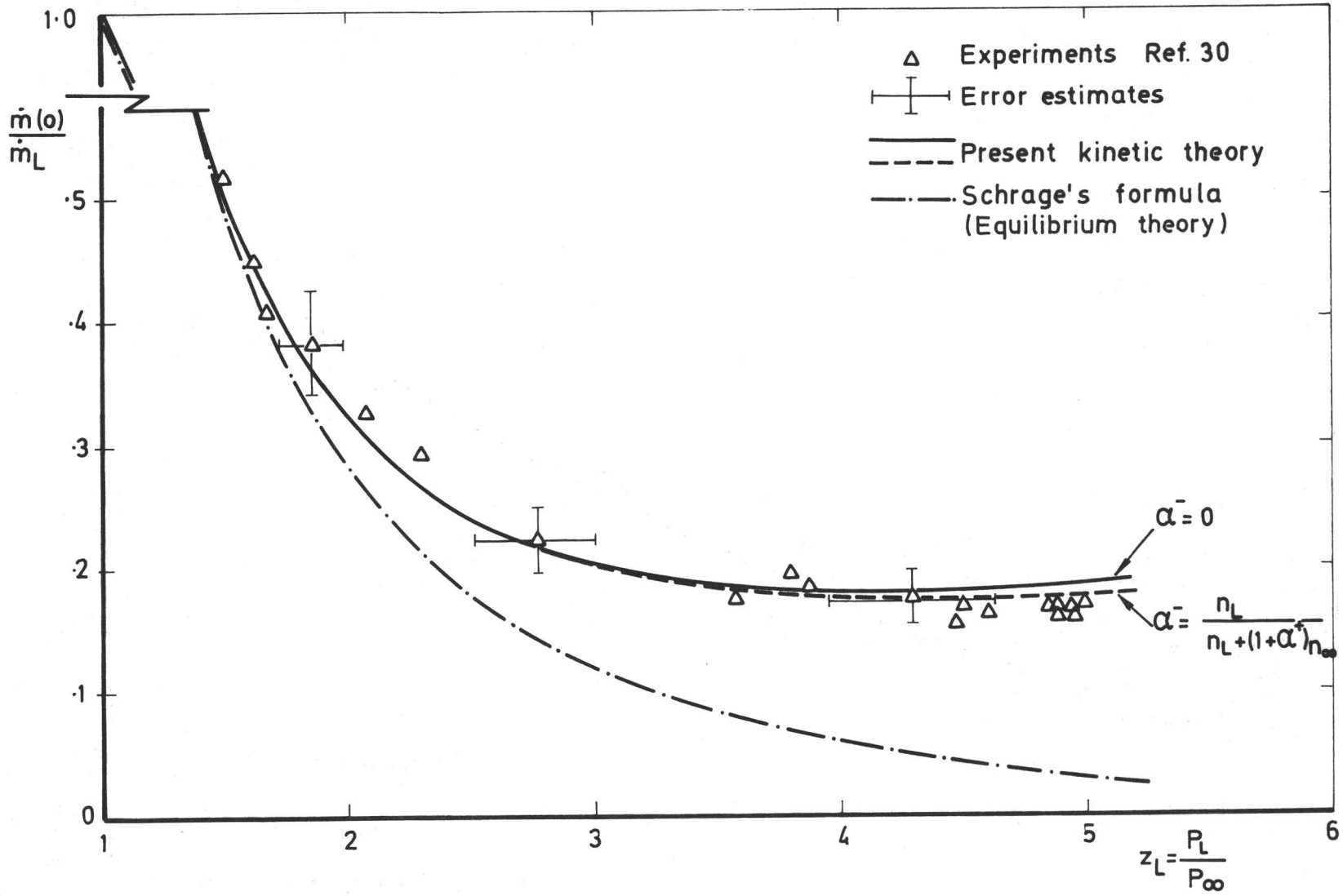

FIG. 15 BACKSCATTERED FLUX TRANSFORMED TO EVAPORATING SYSTEM. COMPARISON WITH EXPERIMENTS

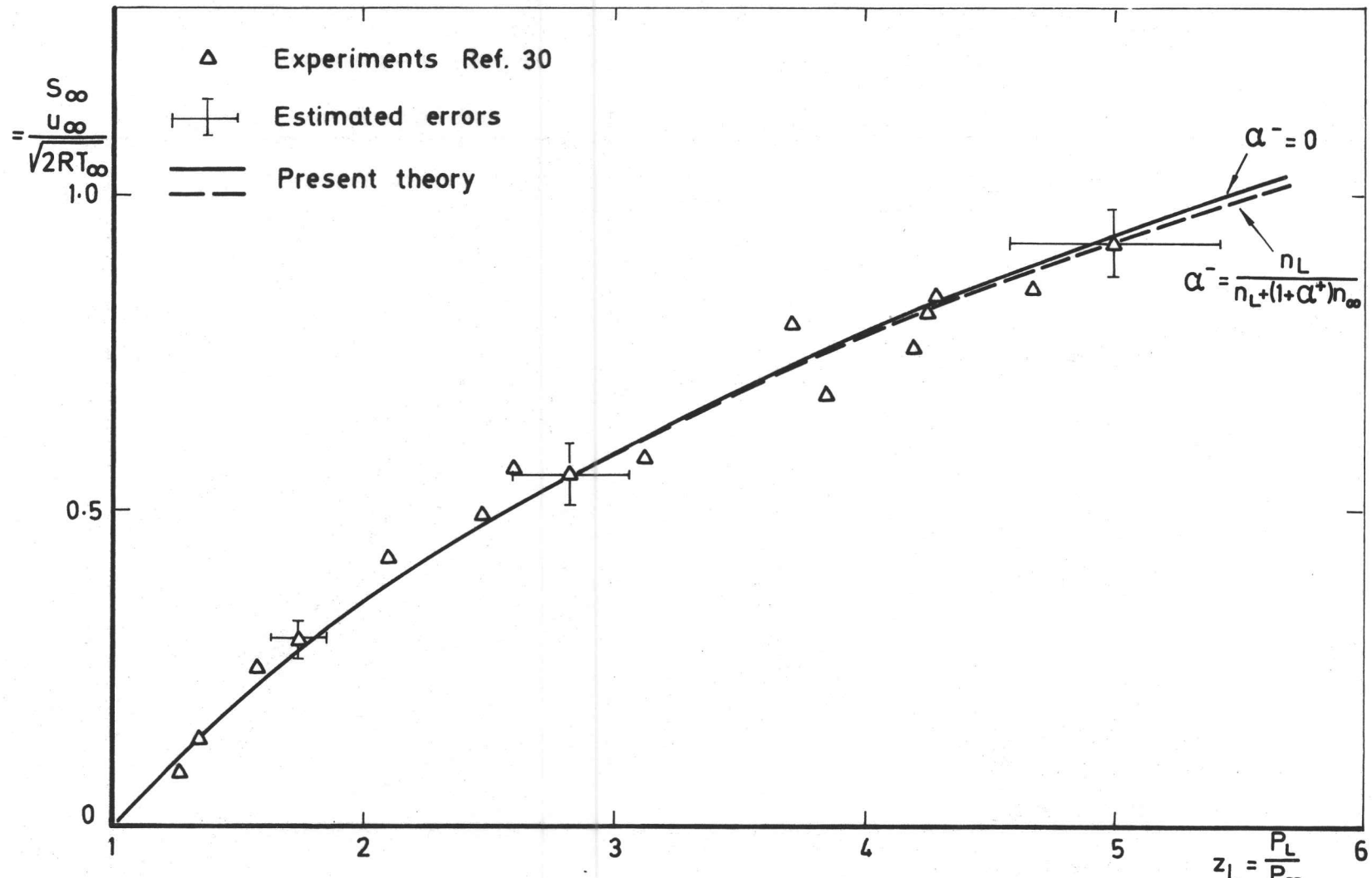

FIG. 16 DOWNSTREAM SPEED RATIO TRANSFORMED TO EVAPORATING SYSTEM COMPARISON WITH EXPERIMENTS

von KARMAN INSTITUTE FOR FLUID DYNAMICS

TECHNICAL NOTE 112

ERRATA :

Fig.10 : The two tables below Fig.10 should be disregarded.

Fig.15 : Ordinate of Fig.15 should read $\dot{m}^{-}(o)/\dot{m}_{L}$